TARGET ASIC-BASED DATA ACQUISITION SYSTEM FOR THE READOUT ELECTRONICS OF THE WATCHMAN DETECTOR

A THESIS SUBMITTED TO THE GRADUATE DIVISION OF THE UNIVERSITY OF HAWAIʻI AT MĀNOA IN PARTIAL FULFILLMENT OF THE REQUIREMENTS FOR THE DEGREE OF

MASTER OF SCIENCE

IN

PHYSICS

DECEMBER 2019

By

Jose Daniel Duron

Thesis Committee:

Gary S. Varner, Chairperson
Kurtis Nishimura
Sven Vahsen

To my parents,

Patricia Colindres and Edgardo Duron,

for your unwavering love and support.

ACKNOWLEDGMENTS

I would like to thank the many members of the Instrumentation Development Laboratory for making this work possible. Special thanks to my advisor, Dr. Gary Varner, for allowing me to work in the IDlab and for his patience in answering my endless questions regarding the TARGET ASIC. I am grateful to Dr. Kurtis Nishimura for lending his expertise to aid the development of firmware. I am thankful for Dr. Sven Vahsen sharing his time and for his guidance in the completion of this thesis.

There are many people that were part of the Hawaii WATCHMAN team. Thank you Ky Ho, Vasily Shebalin, Anthony Schuluchin, Jonathan Hendriks, and Salvador Ventura for your essential contributions which were indispensable for the success of this project. I am very grateful to Oskar Hartbrich an Martin Bessner for sharing their insight and guidance in the making of this thesis. I would also like to thank Brian Crow for his assistance regarding RATPAC simulations. Thank you again to all the members of IDLab whose knowledge and experience were essential for the completion of this thesis.

ABSTRACT

The WATer CHerenkov Monitor for ANtineutrinos (WATCHMAN), is a new detector concept for nuclear non-proliferation monitoring. WATCHMAN will use inverse beta decay reactions in its gadolinium-doped water tank to detect the low energy antineutrinos from nuclear reactions. The detector consists of a 5 kiloton water tank instrumented with around 3600 photomultiplier tubes. This thesis presents the design, simulation and testing of the TARGETC ASIC-based FPGA Mezzanine Card (FMC) Prototype as a demonstration that a TARGET solution will satisfy WATCHMAN's readout requirements. The TARGETC FMC Prototype is a cost-effective data acquisition system that can handle a large number of photomultiplier tubes while digitizing the signals at a high sampling rate. The system uses the TARGETC ASIC, developed by the University of Hawaii as a multi-channel transient waveform digitizer. Employing a commercial System-On-Module with a Zynq-based FPGA, the TARGETC FMC Prototype system offers a self-triggered, dead-time less (at 10 kHz trigger rate), low-cost system compared to commercial alternatives. Simulations of the readout module under 10 kHz dark noise rate are carried out to ensure 100% efficient capture of neutrino inverse-beta decay events.

CONTENTS

LIST OF TABLES

LIST OF FIGURES

CHAPTER 1
INTRODUCTION

The WATer CHerenkov Monitor for ANtineutrinos (WATCHMAN) will use gadolinium(Gd)-doped water to detect low energy anti-neutrinos. The primary aim of WATCHMAN is to demonstrate that neutrinos can be used to passively monitor nuclear reactors for non-proliferation purposes [1]. WATCHMAN will use inverse beta decay reactions inside its active water volume to detect the reactor antineutrinos [1]. An antineutrino undergoes inverse beta decay when it interacts with a quark in a proton of a hydrogen nucleus producing a positron and converting the proton into a neutron [2]. A prompt signal is generated by the positron when it annihilates with an electron. A second, delayed signal, is the result of energy being released after the neutron capture by a gadolinium or hydrogen nucleus. The method of antineutrino detection is the coincidence of a prompt and delayed signal from an inverse beta decay event.

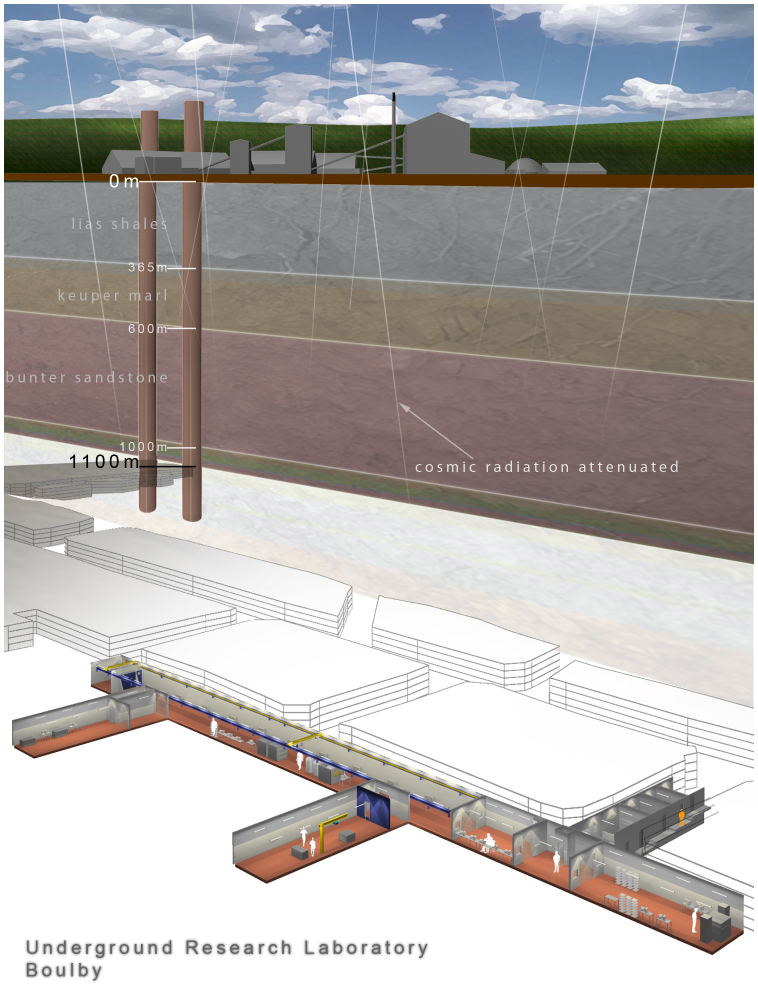

Figure 1.1: Boulby Underground Laboratory [3]

The detector will be built in the Boulby Mine under 1,100 meters of rock (Fig. 1.1), near Boulby, United Kingdom [3]. The site is located 25 km away from the Hartlepool nuclear power station, which will serve as the source of the reactor neutrinos. The cylinder shaped tank will be a part of the existing Boulby Underground Laboratory. The tank will be 20 meters high and 20 meters in diameter, containing 5 kilotons of Gd-doped water. WATCHMAN will use around 3,600 254 mm diameter photomultiplier-tubes (PMTs) to detect photons generated inside the tank (see Figure 1.2).

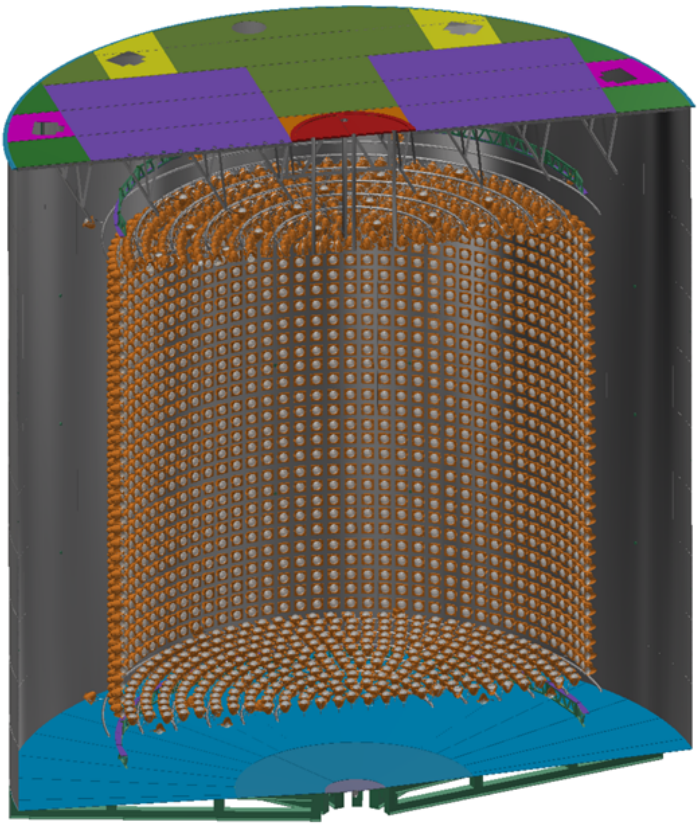

Figure 1.2: WATCHMAN Tank Conceptual Design [3]

1.1 WATCHMAN Project Goals

The main goal for WATCHMAN consists of monitoring the activity of nuclear reactors. Specifically, WATCHMAN will have the ability to confirm the existence of an operating reactor and determine the operational status of the power plant. WATCHMAN will allow the next generation of U.S. and U.K. scientists and nuclear-policy experts an opportunity to develop, operate and analyze results from nonproliferation technology deployments as well as collecting data for future research and analysis for antineutrino-based detection[3]. In the future, this detector can also be used as a testing ground for new emerging technologies such as Water Based Liquid Scintillators (WbLS) and Large Area Picosecond Photodetector (LAPPD) [3].

WATCHMAN seeks to add to the number of detectors around the world such as KAMLAND [4], JUNO [5], and Daya Bay [6], among others, that can detect reactor antineutrinos. Hartlepool Nuclear Power Plant will operate until 2024, when it is expected to shut down. The expected lifetime of the WATCHMAN detector is 10 years. Even after the reactors are powered down,

WATCHMAN can still provide important information regarding backgrounds [3]. Additionally, WATCHMAN has scientific merit for studying supernova neutrinos due to its ability to measure the direction of incoming neutrinos. Once built, WATCHMAN would be the largest supernova neutrino detector in the western hemisphere [1].

1.2 WATCHMAN Readout and DAQ Subsystem

WATCHMAN requires a readout and data acquisition (DAQ) system that will fulfill the project goals. To this end a DAQ subsystem group was convened to formulate a solution for WATCHMAN. The DAQ subsystem group consists of two parts, a hardware electronics group and a software group. Three universities make up the core of the WATCHMAN DAQ hardware group, Pennsylvania State University, Iowa State University and University of Hawaii. Each university is set to present a readout and DAQ system solution for WATCHMAN. From these three proposed systems, the most cost-effective system that meets all requirements will be implemented as the final WATCHMAN readout system. From the University of Hawaii, the Instrumentation and Development Lab (IDLab) was purposed to develop a design for a suitable readout system.

This thesis presents the development of a DAQ system prototype for WATCHMAN. The second chapter explores on the physics behind the reactor antineutrinos, the method of detection, and the photodetectors utilized. The third chapter illustrates WATCHMAN's functionality, based on detector simulations using GEANT4 [7] and RAT-PAC [8]. The fourth chapter details the requirements for the DAQ system. The DAQ prototype design is explained in detail in chapter five. The results of this prototype are summarized in chapter six. Chapter seven discusses the next step in development for the proposed DAQ system. Chapter eight discusses the viability of the proposed DAQ hardware as a solution for WATCHMAN's readout system.

CHAPTER 2
PHYSICS OF WATCHMAN AND INVERSE BETA DECAY NEUTRINO DETECTION

2.1 Reactor Antineutrinos

The process by which nuclear reactors produce antineutrinos is beta decay. Beta decay is a process where a bound neutron in a neutron-rich nucleus will undergo a reaction by changing into a proton and emitting an electron and an electron antineutrino [9]. This interaction is described in equation 2.1 below:

$$n \rightarrow p + e^{-} + \overline{v}_{e} \tag{2.1}$$

Nuclear reactors use the fission of ^{235}U as the main fuel source to generate energy. Free neutrons from the reaction can be captured by ^{238}U present in the fuel source, in turn producing two other isotopes ^{239}Pu and ^{241}Pu [9]. After neutron capture, ^{238}U produces electron antineutrinos as it beta decays into ^{239}Np and then ^{239}Pu. ^{235}U, ^{239}Pu, and ^{241}Pu also produce electron antineutrinos through the beta decay of their fission products. Fission of ^{238}U requires higher energy neutrons, around 1 MeV, and its products can also beta decay, producing antineutrinos. The energy spectrum of reeactor neutrinos from these four isotopes is detailed in Figure 2.1. High power reactors produce around 2×10^{20} antineutrinos isotropically per second for each gigawatt (GW) of thermal power. [9]. The Hartlepool power plant has two reactors each producing 1.5 GW of thermal power [3].

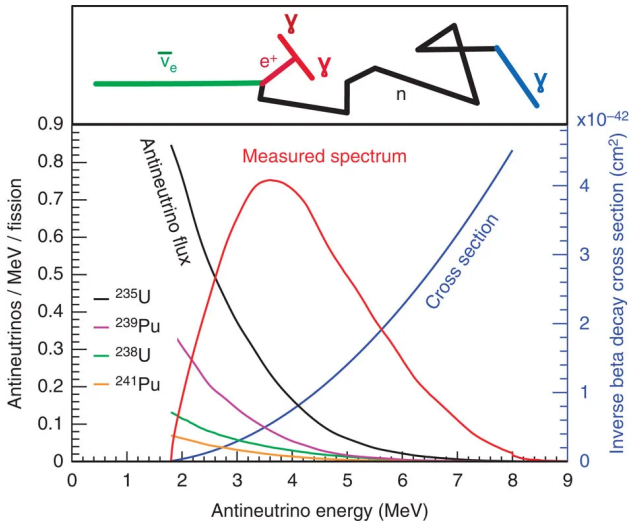

Figure 2.1: Antineutrino energy spectrum from the fission products of ^{235}U, ^{238}U, ^{239}Pu, and ^{241}Pu, the inverse-beta decay cross section, and the measured spectrum. The upper section describes the inverse beta decay interaction.[3].

2.2 Inverse Beta Decay (IBD)

Antineutrinos can be detected through the Inverse Beta Decay (IBD) process:

$$\overline{\nu}_e + p \rightarrow e^+ + n \tag{2.2}$$

Antineutrinos react with the protons (hydrogen nuclei) in water molecules to produce a positron and a neutron. Through the inverse beta decay process, antineutrinos generate two signals, one immediately from the from the positron when it annihilates with an electron, and a second delayed response as the neutron is captured by gadolinium after it loses energy through elastic collisions with protons in the water [9]. The delayed signal will happen approximately 30 microseconds after the prompt signal with .01% gadolinium concentration [3]. The gamma-rays emitted by the neutron capture can transfer energy and accelerate nearby electrons that will emit Cherenkov radiation [3]. This distinct signature of the coincidence of two separate signals is a very useful feature because it helps distinguish an IBD event from other background signals. The energy of the antineutrino can be approximated to the energy of the prompt signal using energy conservation.

Using energy conservation on the Inverse Beta Decay reaction yields:

$$E_{\overline{\nu}_e} + E_{proton} = E_{positron} + E_{neutron} \tag{2.3}$$

The energy of the proton, E_{proton}, with natural units is represented as $T_{proton} + m_{proton}$, the kinetic energy of the proton plus the mass of the proton respectively. Similarly, the energy of the neutron, $E_{neutron}$, is expressed as kinetic energy of the neutron, $T_{neutron}$, plus the mass of the neutron, $m_{neutron}$. Substituting these expressions into equation 2.3 results in:

$$E_{\overline{\nu}_e} + T_{proton} + m_{proton} = E_{positron} + T_{neutron} + m_{neutron} \tag{2.4}$$

Assuming the proton is at rest, ($T_{proton} = 0$), and solving for $E_{\overline{\nu}_e}$, the equation approximates to:

$$E_{\overline{\nu}_e} \approx E_{positron} + T_{neutron} + m_{neutron} - m_{proton} \tag{2.5}$$

Energy conservation applied to the electron-positron annihilation results in:

$$E_{vis} \approx E_{positron} + m_{electron} \tag{2.6}$$

The visible energy, E_{vis}, is equal to the energy of the positron and the mass of the electron. Substituting 2.6 into 2.5 and solving for $E_{\overline{\nu}_e}$ yields:

$$E_{\overline{\nu}_e} \approx E_{vis} + m_{neutron} - m_{proton} - m_{electron} + T_{neutron} \tag{2.7}$$

Using the current world average values for $m_{neutron}$, m_{proton}, and $m_{electron}$from the Particle Data Group [10], the energy of the neutrino, $E_{\overline{\nu}_e}$ can be related to signal from the positron-electron annihilation and the kinetic energy of the neutron:

$$E_{\overline{\nu}_e} \approx E_{vis} + .78MeV + T_{neutron} \tag{2.8}$$

The energy of the delayed signal, which comes from the neutron capture is smaller, around tens of keV, when compared to the energy of the antineutrino [9]. Gadolinium has the highest neutron capture cross section of all elements. Gadolinium is used to increase the photon yield of the neutron capture as it yields more photons than a neutron capture through hydrogen and reduces the capture time[9]. Neutron capture by a hydrogen nucleus takes around 200 microseconds compared to around 30 microseconds with gadolinium [11]. This method of detecting antineutrinos is shown in Figure 2.2. The gamma ray photons from both types of signals will transfer energy to nearby electrons that will accelerate and emit Cherenkov radiation.

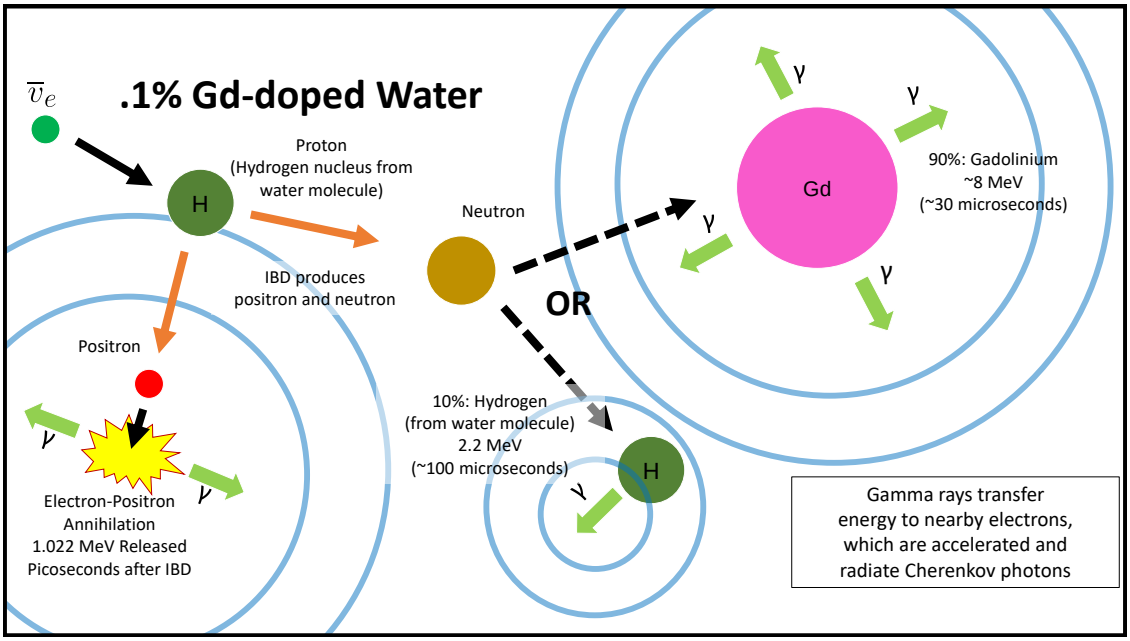

Figure 2.2: Inverse Beta Decay as a antineutrino detection method with Gd-Doped Water [9]

2.3 Photodetectors

The Cherenkov photons generated by the IBD can be detected by sensitive photodetectors. The walls of the WATCHMAN tank will be lined with about 3600 photomultiplier tubes (PMTs), which convert Cherenkov photons from the IBD events. In order to be able to reconstruct an IBD event, the signals from many PMTs must be collected and processed. WATCHMAN requires a DAQ system employing high-speed, multichannel analog-to-digital converters to collect data from all the PMTs.

Figure 2.3: Hamamatsu R7081-100 PMT [12]

The photodetectors of choice are the Hamamatsu Large Photocathode Area PMT model R7081-100. This PMT has a diameter of 253 mm with a surface area of 470 cm^2. The spectral response ranges from 300 nm to 650 nm, with the peak efficiency at a wavelength of 470 nm. This spectral response covers the Cherenkov radiation spectrum in water as shown in Figure 2.4. Cherenkov radiation wavelength in water peaks at 375 nm [13]. The R7081-100 PMT has a quantum efficiency of 35% for wavelengths of 390 nm [12]. The typical gain ranges around 1.0×10^7 with a supply voltage of 1500 volts [12]. These PMTs have a single channel output. The PMT specifications determine many of the design requirements for the data acquisition system. Among the more important characteristics of this PMT is the rise time of the output pulse. The output of the PMT has a rise time of 3.8 ns [12]. Another important characteristic is its intrinsic noise rate, called dark noise. Due to the low energies associated with the IBD prompt and delayed signals, it is imperative to retain sensitivity to the smallest possible outputs from the PMT, which have the same magnitude as the dark noise, due to photocathode thermal emission. The only way to differentiate between a single photoelectron signal from an IBD event and dark noise is that an IBD event has a coincidence of multiple PMT hits in a time window. In contrast the PMT dark noise is randomly distributed. For this particular model, the PMT dark count rate is typically 8 kHz with a maximum rate of 16 kHz.

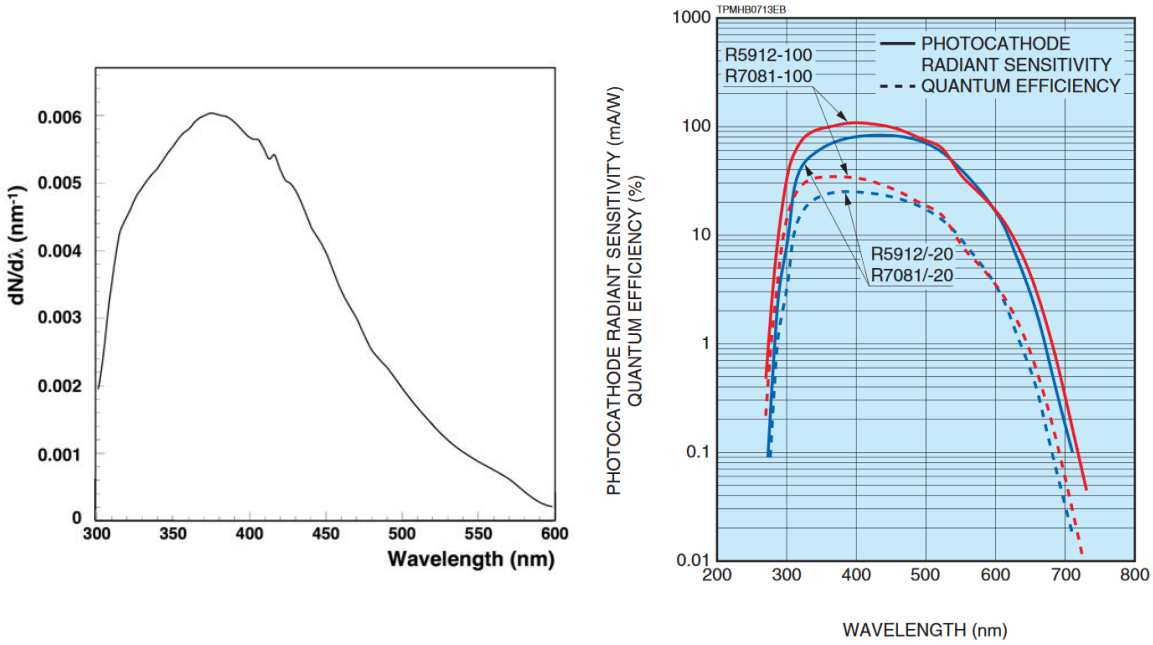

Figure 2.4: Cherenkov radiation spectrum in water [13] (left). Hamamatsu R7081-100 (red) Photocathode Sensitivity and Quantum Efficiency [12] (right).

CHAPTER 3
WATCHMAN DETECTOR EVENT SIMULATIONS

3.1 RAT-PAC and GEANT4

In order to understand WATCHMAN as a detector, a series of simulations have been carried out [3]. A software tool called RAT-PAC, (Reactor Analysis Tool Plus Additional Codes), generates reactor signals and backgrounds [8]. RAT-PAC uses GEANT4 [7] and GLG4sim [14] to simulate how particles propagate in gadolinium-doped water and it also models the photons resulting from the particle interactions. RAT-PAC has a virtual DAQ system that determines if an event would generate a trigger.

The WATCHMAN software group has incorporated the WATCHMAN detector structure, including geometry, and PMT type into RAT-PAC. It takes into account the rock surrounding the detector, the concrete walls, the PMT support structure and the PMT cables. The simulated detector is 99.9% water and 0.1% gadolinium. The current geometry in RAT includes 3554 PMTs, 3257 inner PMTs and 295 outward facing veto PMTs. The tank has a diameter of 20 meters and is 20 meters tall. Figure 3.1 shows an image of the WATCHMAN detector geometry generated by RAT-PAC.

The goal of the simulation studies presented in this chapter is to understand the requirements for the WATCHMAN DAQ system. It is possible to ascertain the minimum readout specifications needed to reliably reconstruct an IBD event. The effect of dark noise on the number of PMT hits is also examined. Additionally, muons are simulated to gain an understanding of the impact that a muon traversing through the detector will have on the DAQ system.

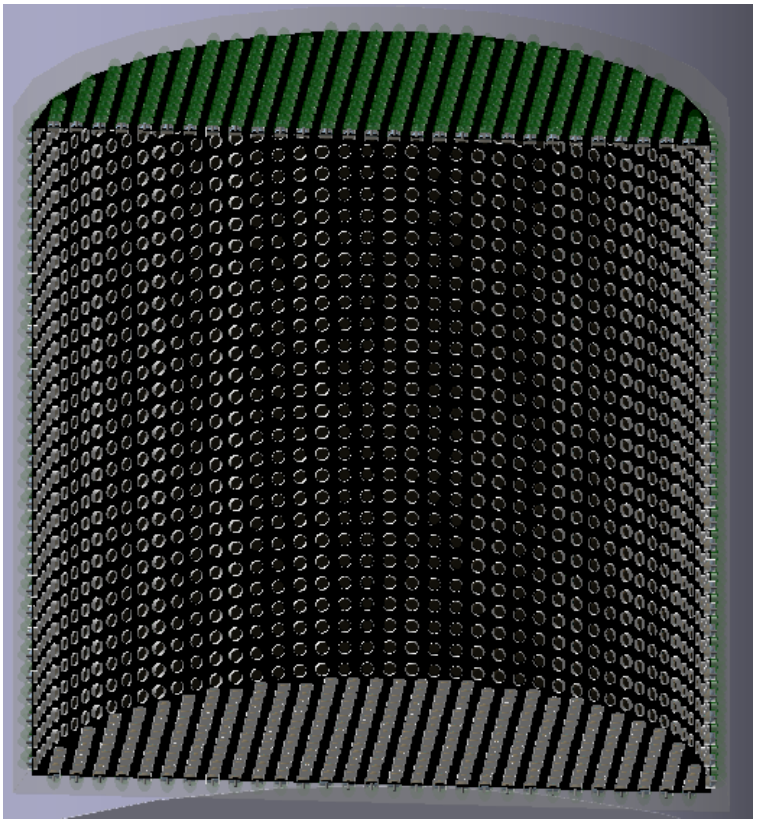

Figure 3.1: Visualization of the WATCHMAN detector geometry implemented in RAT-PAC.

3.2 Event Generators

RAT-PAC depends on GLG4sim to generate physics events. The generators have many useful parameters that can be configured freely. The gun generator was used to carry out all the simulations in this thesis. Gun was chosen because it allows direct control over the the initial position of a particle as well as its direction and energy. This generator also allows the initial position to be set uniformly in a volume. This feature was used to generate events throughout the inside of the detector.

3.3 PMT Model

RAT has a model for the Hamamatsu R7801 PMT. The software loads a table with the position and direction of every PMT. The PMT photocoverage is about 25% of the surface area of the detector. Probability density functions (PDFs) for single photoelectron charge and transit time are used to produce a realistic response to a photon being detected by a photocathode [8]. The PDFs

for charge time and transit time for the R7801 PMT are shown below in Figure 3.2. The model for the PMT does not include dark noise. Dark noise is simulated separately in the event builder module discussed in the Event Processor section.

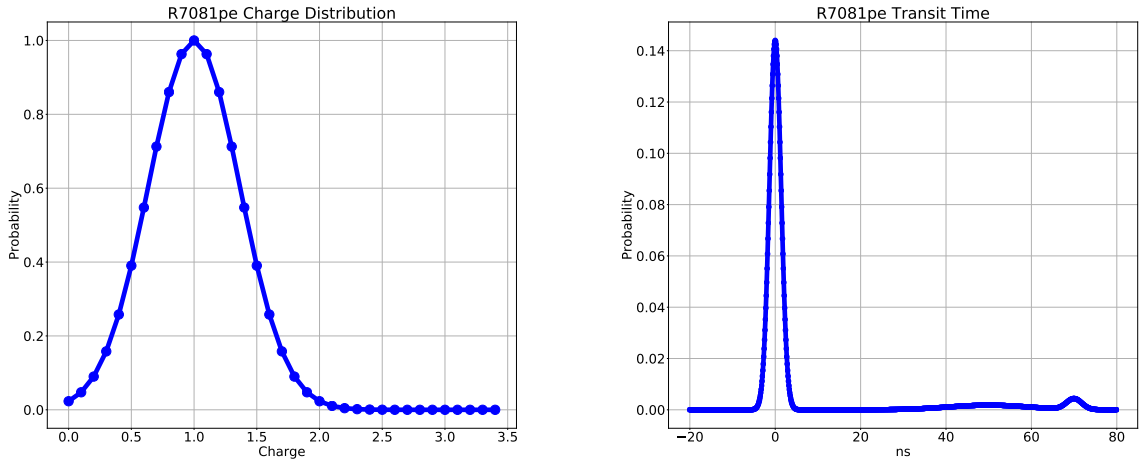

Figure 3.2: PDF of R7081pe charge distribution for single photoelectron hits (right). Transit time PDF used to simulate signal delay, with a second peak for afterpulses (left).

3.4 Virtual DAQ System

The virtual DAQ will create a timestamp the moment a PMT is hit by a photon. The timestamp of the hit corresponds to the first photon hitting the PMT plus the PMT's transit time. The charge of the PMT is the total charge accumulated by the PMT regardless of the time it took to accumulate [8]. The virtual DAQ creates a timestamp, calculates the total charge, and records the location of all PMTs that were hit by photons for every Monte Carlo event.

3.5 Event Processors

RAT-PAC includes tools that will process the raw simulation data called event processors. The tools used to process the simulation outputs were FitCentroid and BONSAI, (Branch Optimization Navigating Successive Annealing Iterations)[15]. Both of these processors taken together were used to rebuild a physics interaction based on the timestamp, charge and number of PMT hits in an event. The minimum number of hits per detector event was set to four PMT hits. BONSAI also adds simulated PMT dark noise. Dark noise was simulated at a 10 kHZ rate using a Poisson trigger. The output of BONSAI includes the reconstructed detector events' vertices position and direction,

as well as the trigger time, number of p.e. per event and number of PMT hits per event. In Table 3.1 the main parameters specified for detector event reconstruction are listed. Reconstructed detector events are not the same as physics events. One Monte Carlo simulation for an IBD event can generate two reconstructed detector events, where the prompt and the delayed signal are two separate detector events.

Table 3.1: BONSAI Parameters

PMT time resolution	1.00 ns
PMT coincidence time difference	1.00 ns
Minimum Number of PMT hits	4
Minimum wall distance for 4-hit vertices	1000 mm
PMT dark noise rate	10 kHz

3.6 Inverse Beta Decay

In order to simulate inverse beta decay physics events, RAT-PAC has a reactor antineutrino generator. This reactor antineutrino generator produces a positron and a neutron pair for every Monte Calro event as shown in Figure 3.5. The energy of the positron and neutron depends on initial energy of the neutrino energy based on a PDF total neutrino flux from a reactor and the inverse beta-decay cross-section [8]. A histogram of the initial energy of the Monte Carlo particles is shown in Figure 3.3 below. It is possible to specify where in the detector the particles will be created. Inverse beta decay simulations were carried out with 10,000 Monte Carlo events uniformly distributed inside the detector.

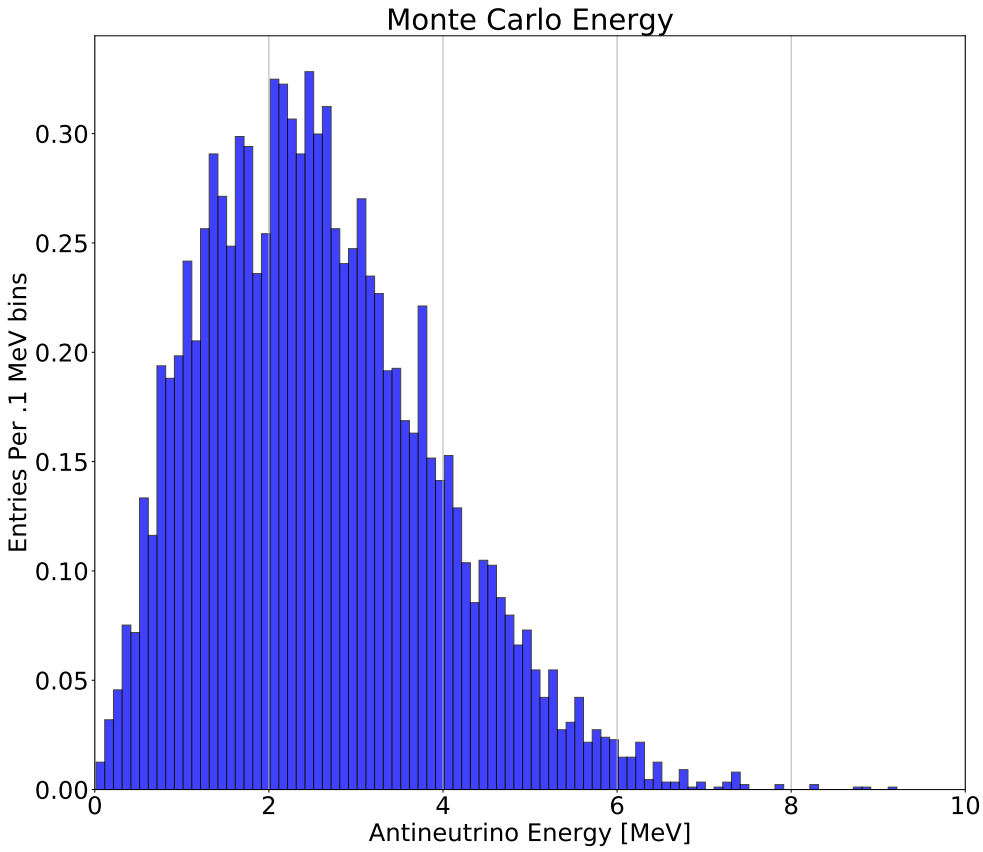

Figure 3.3: Antineutrino energy histogram for 10,000 Monte Carlo Reactor IBD Events.

The positron will annihilate with the electron and the gamma rays will transfer their momentum to nearby electrons which will then emit Cherenkov radiation. The neutron will be losing kinetic energy until it can be absorbed by a hydrogen nucleus or a gadolinium nucleus, in turn creating gamma rays that will accelerate electrons again emmiting Cherenkov photons. IBD events on average generate around 2350 Cherenkov photons, as shown in Figure 3.4. The Cherenkov photons are propagated through the water volume until they are either absorbed by the water, the tank wall or hit a PMT. If they reach a PMT surface then the virtual DAQ will register a hit after taking into account quantum efficiency. The virtual DAQ will create a timestamp, and store the accumulated charge for each hit.

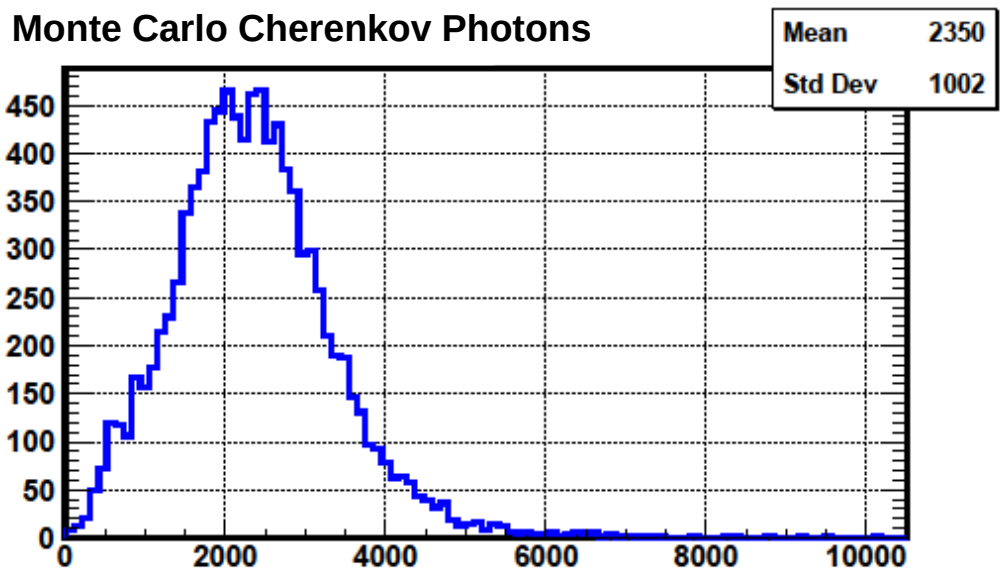

Figure 3.4: Number of Cherenkov photons generated per IBD Event for 10,000 Monte Carlo simulations.

3.6.1 Reconstruction of IBD Events using BONSAI

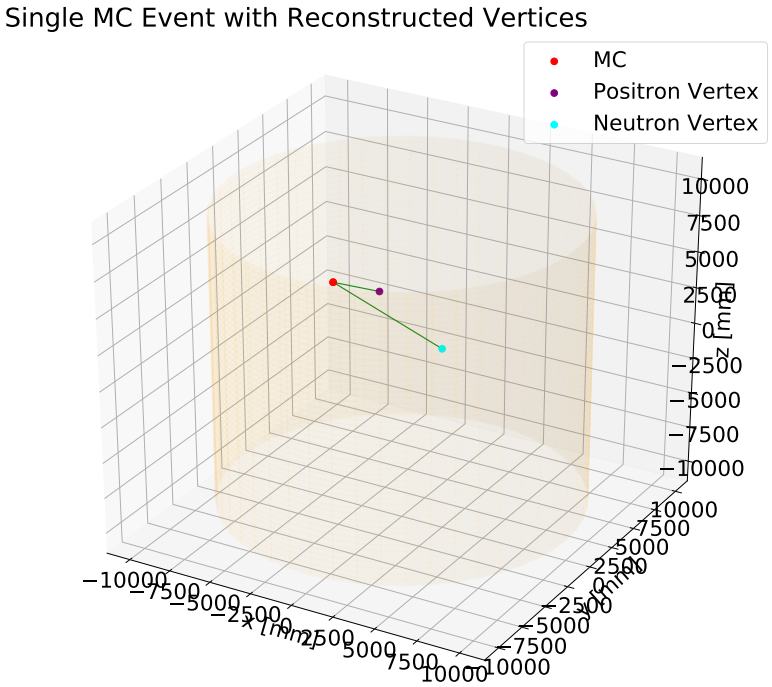

Figure 3.5: Reconstructed Inverse Beta Decay event in WATCHMAN detector, simulated using RAT-PAC, with the initial MC position (red), the positron vertex (purple) and the neutron capture vertex (blue).

The simulated raw data was processed using BONSAI. BONSAI finds clusters of PMT hits and reconstructs the vertices of the Cherenkov cone. In Figure 3.5, above, the red marker is the initial Monte Carlo position of the IBD event, the purple marker is the reconstructed vertex of the positron and the light blue maker is the vertex of the neutron capture.

Simulations with 10,000 Monte Carlo IBD events uniformly distributed inside the detector were carried out and reconstructed. The simulation uses the same reactor neutrino energy spectrum for the initial Monte Carlo energy for all the events.

A heat map showing the position of all the reconstructed vertices is shown in Figure 3.6. All the reconstructed events are inside a cylinder with a diameter of approximately 15.4 meters and a height of 14.4 meters. This is a feature of BONSAI where no events are reconstructed at close proximity to the PMT walls.

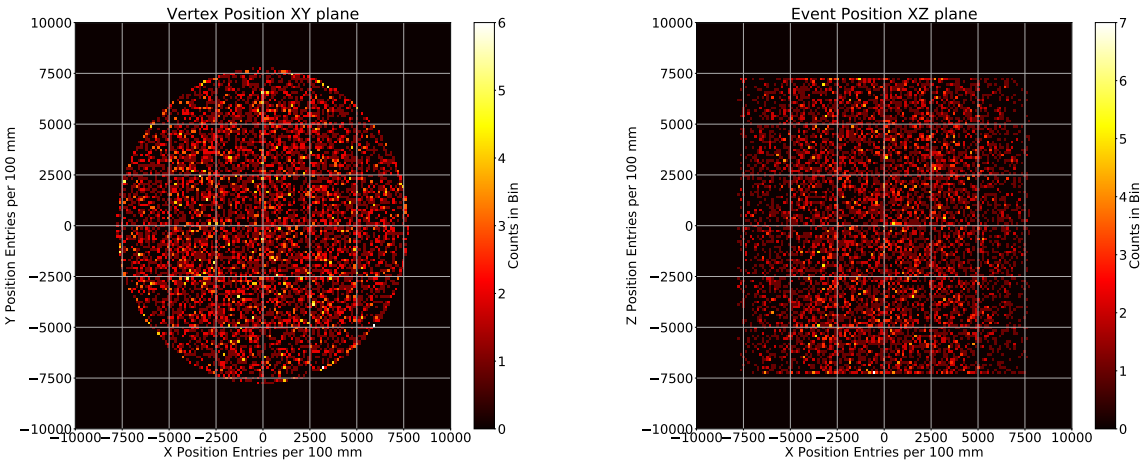

Figure 3.6: A density map of the reconstructed vertices in the XY (right) and the XZ plane (left).

The p.e. distribution per event was plotted against the number of PMT hits per event as shown in Figure 3.7. One of the main challenges for the DAQ system is the relatively low amount of p.e. per PMT. Most hits are single p.e. hits for both the prompt signal from the positron and the delayed signal from the neutron. There are fewer Cherenkov photons created than the number of PMTs in the detector.

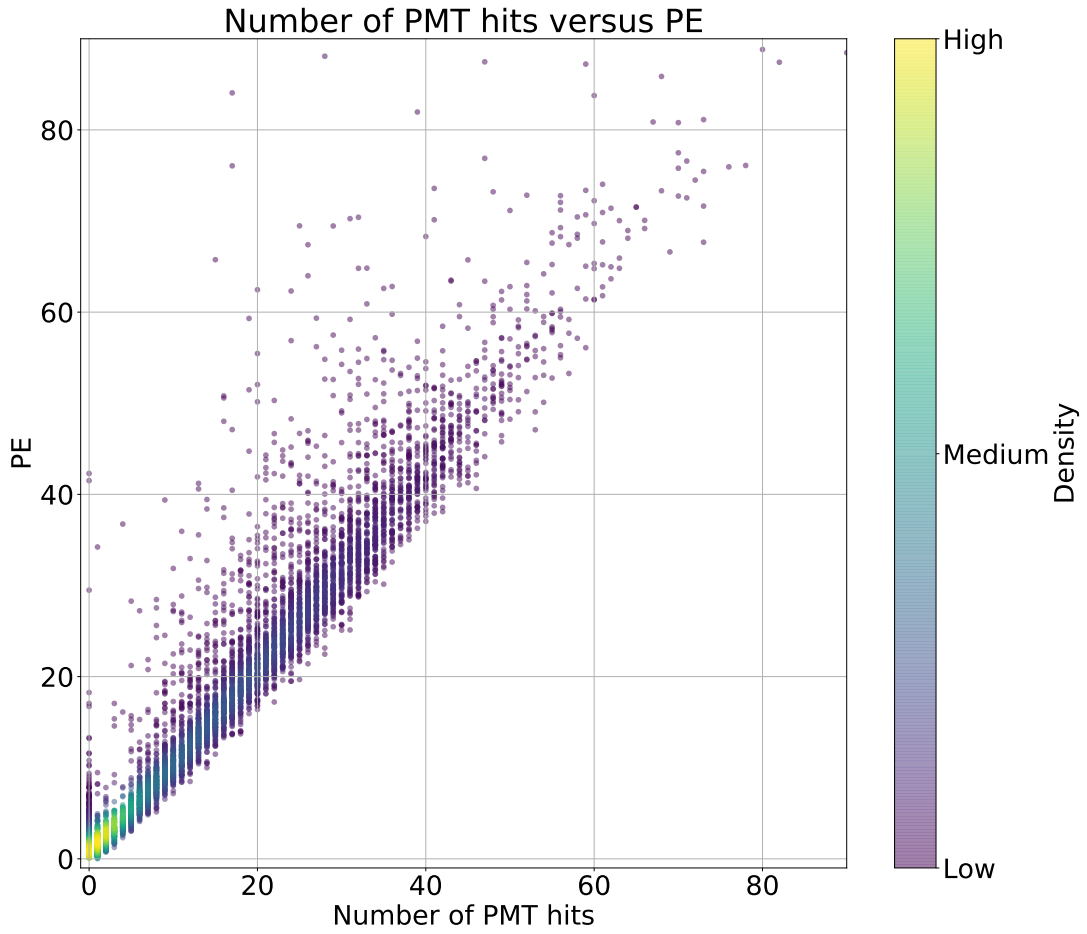

Figure 3.7: Number of p.e. per IBD event.

It is possible to determine the particle that produced the signal by looking at the trigger time. Figure 3.8 shows a histogram of the distribution of event trigger time. The positron-electron annihilation prompt signal takes place within 10 to 100 nanoseconds after an inverse beta decay interaction. The delayed signal due to neutron capture is significantly slower, starting at 1 microsecond and up to 100 microseconds. The considerably larger triggered time range for the neutron makes sense because the neutron needs to lose kinetic energy, mostly from elastic collisions with hydrogen nuclei in the water, before it can be captured by a nucleus.

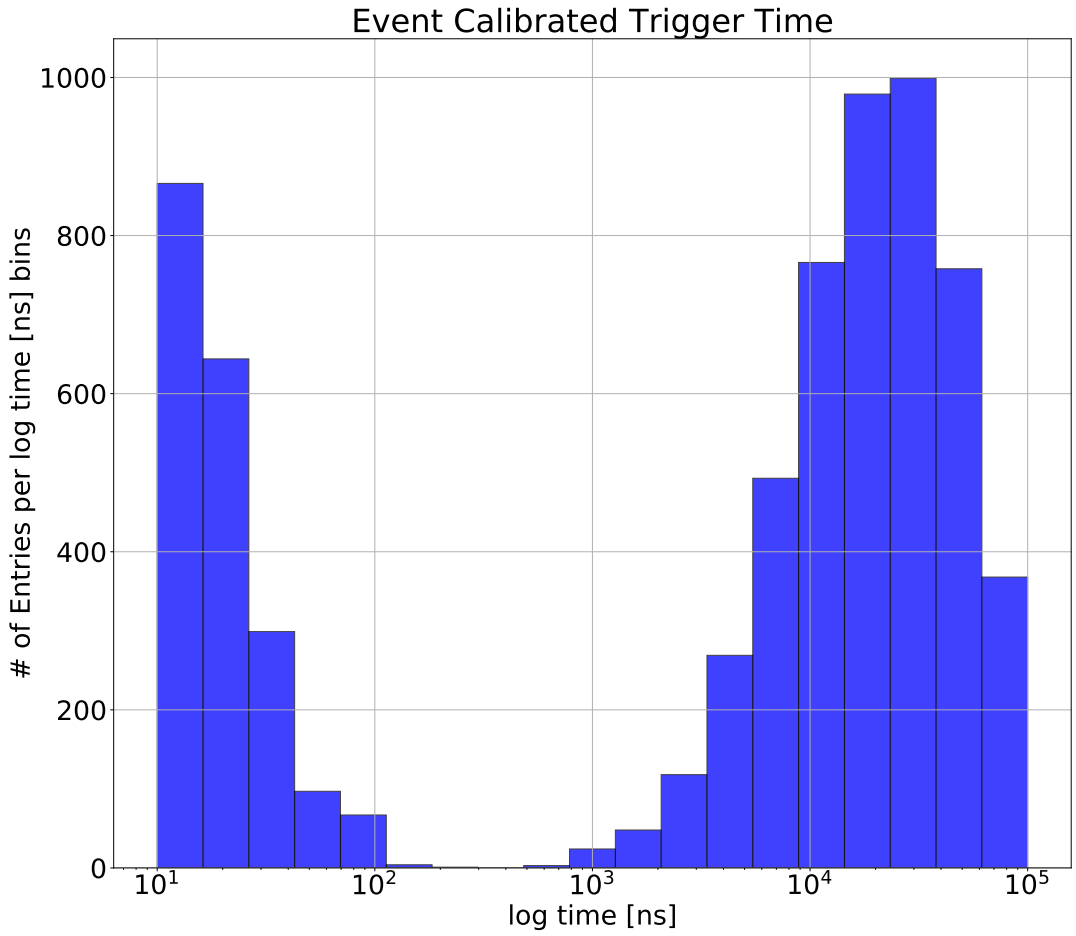

Figure 3.8: Distribution of trigger timestamp for all events.

Proper time-stamping of the events is important because both signals have similar range of total charge (p.e.) demonstrated by Figure 3.9. The prompt and delayed signal cannot be identified in terms of charge. The time referred here is the time from the Monte Carlo simulation generated the positron and neutron pair to when the virtual DAQ registered a hit on the PMT.

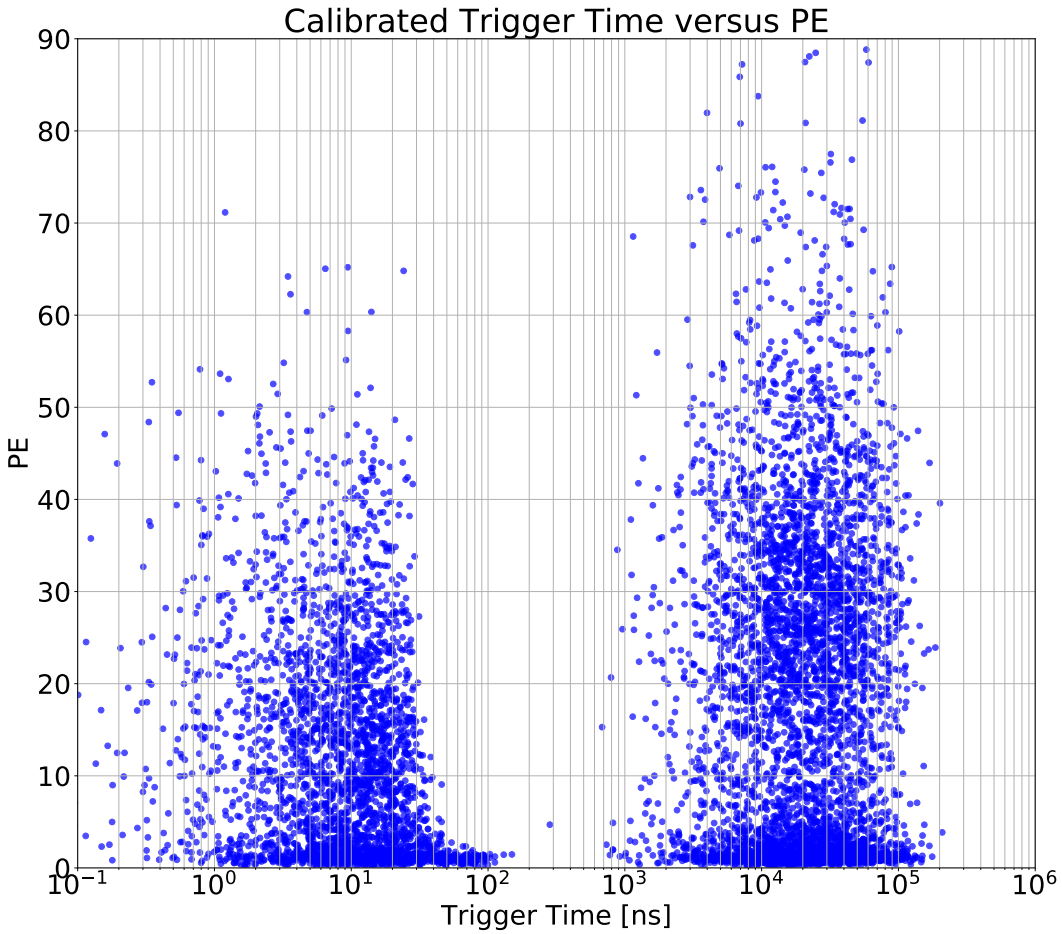

Figure 3.9: Trigger time versus total charge of all reconstructed events.

Dark rate noise is an important aspect to consider for the DAQ system. Most hits from IBD events are single p.e. hits and for reconstruction every hit is important. The thermal noise from the PMTs causes single p.e. hits that cannot be distinguished from a hit from an IBD event. To understand how dark noise will affect the reconstruction process, dark noise with a Poisson rate of 10 kHz was simulated for each PMT. In Figure, 3.10, the total number of PMT hits including simulated dark noise is shown.

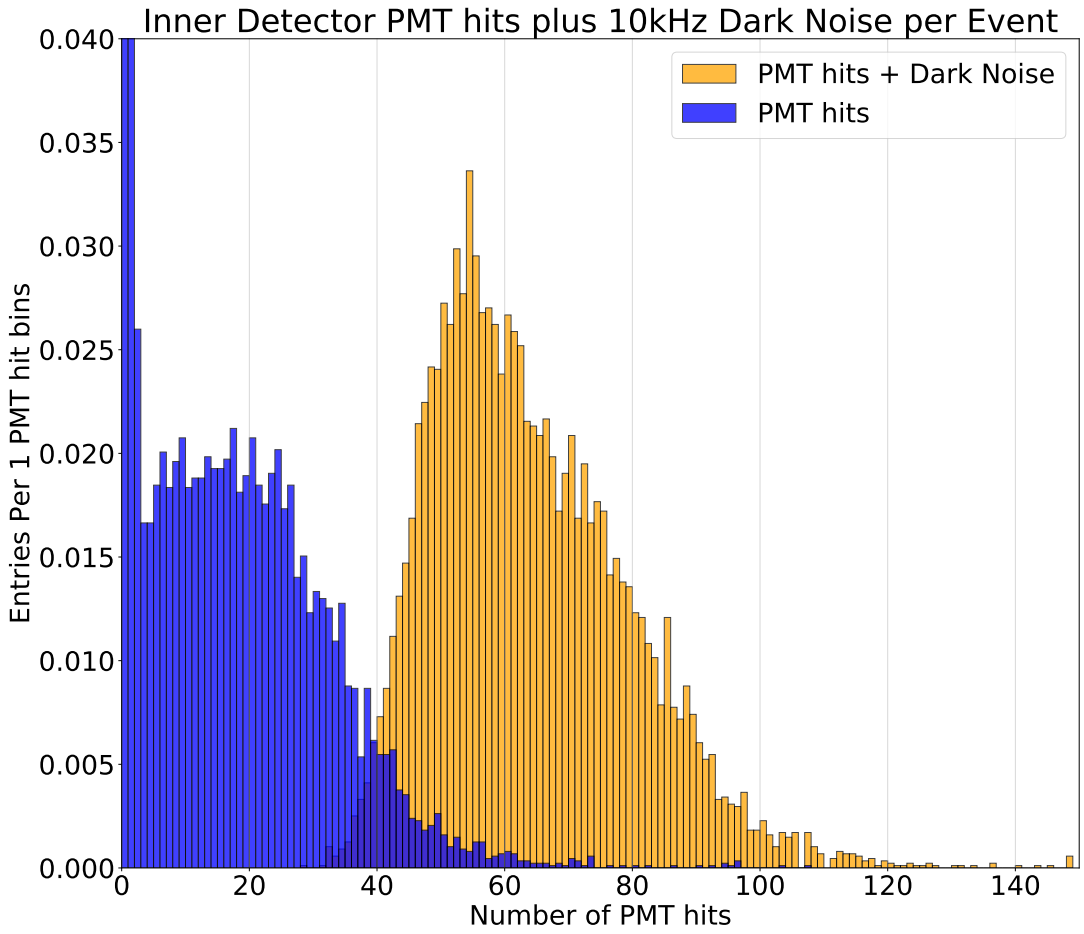

Figure 3.10: Number of PMT Hits per event plus 10 kHz Dark Noise rate.

3.7 Muons

Muons are a significant background due to the amount of photons that they generate inside the detector. The muon rate is also significantly higher than IBD, around 0.1 Hz versus 1.7 IBDs per day. A particle gun was set up with muons as the particle. 800 MeV was specified as the energy of the muon. The gun was set up so that all the muons' trajectory is downwards with the initial position being distributed uniformly on a disk on top of the detector. In Fig 3.11, the number of Cherenkov photons simulated by each event is shown. Due to high computational resource utilization by RAT when simulating and tracking all the Cherenkov photons, higher energy muon event simulations that would create larger amounts of Cherenkov photons were unable to be

simulated.

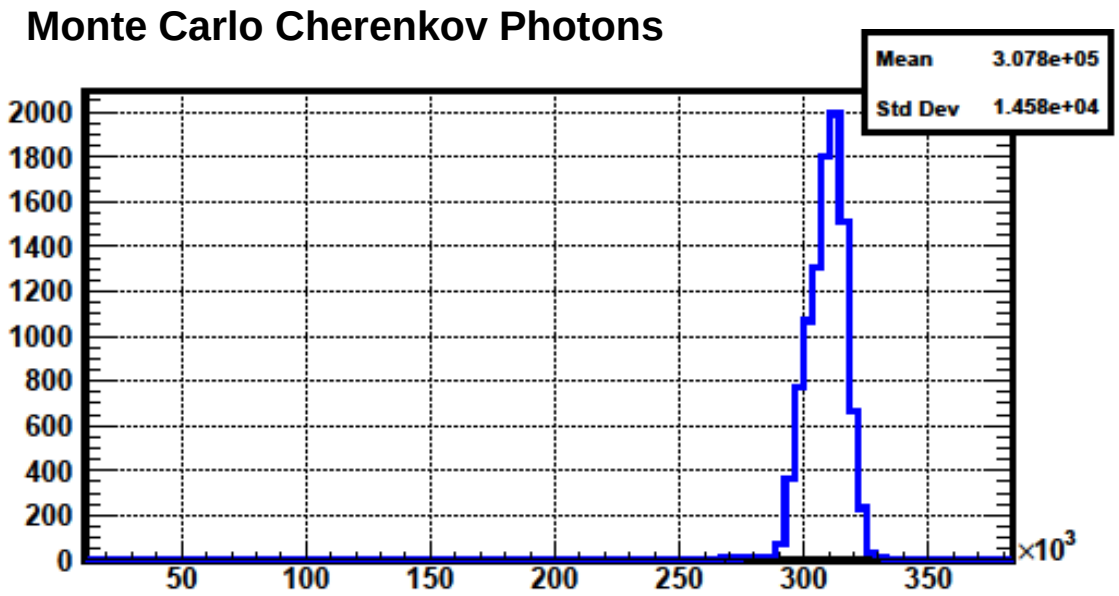

Figure 3.11: Number of Cherenkov Photons per 800 MeV Muon event.

The distribution of reconstructed vertices of the muon events is shown in Figure 3.12. The muons immediately radiate Cherenkov photons upon entering the detector from the top.

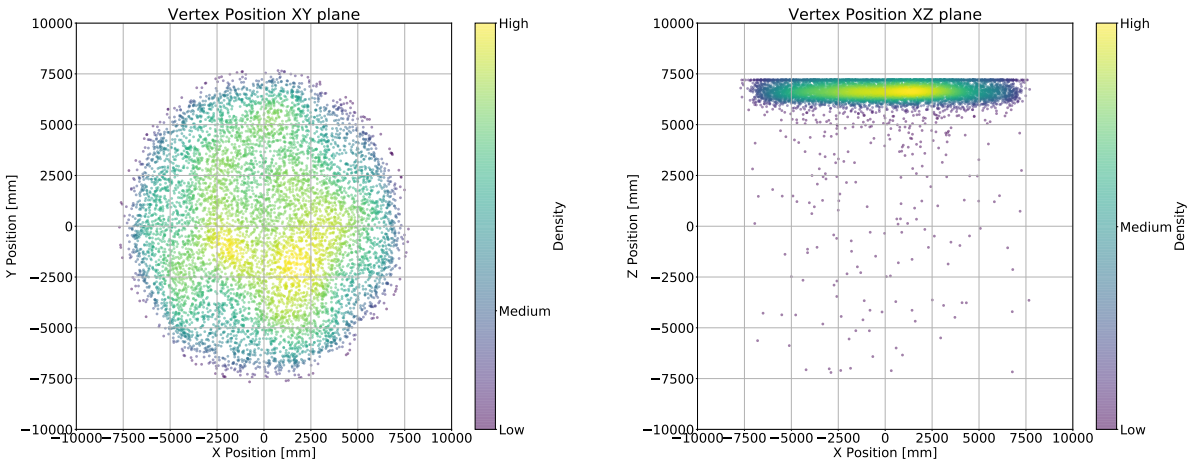

Figure 3.12: A density map of the reconstructed vertices in the XY (right) and the XZ plane (left).

Muons deposit a much larger amount of charge on the PMTs and hit a much higher number of PMTs. In Figure 3.13 , the number of p.e. per event is plotted against the number of PMT hits per event.

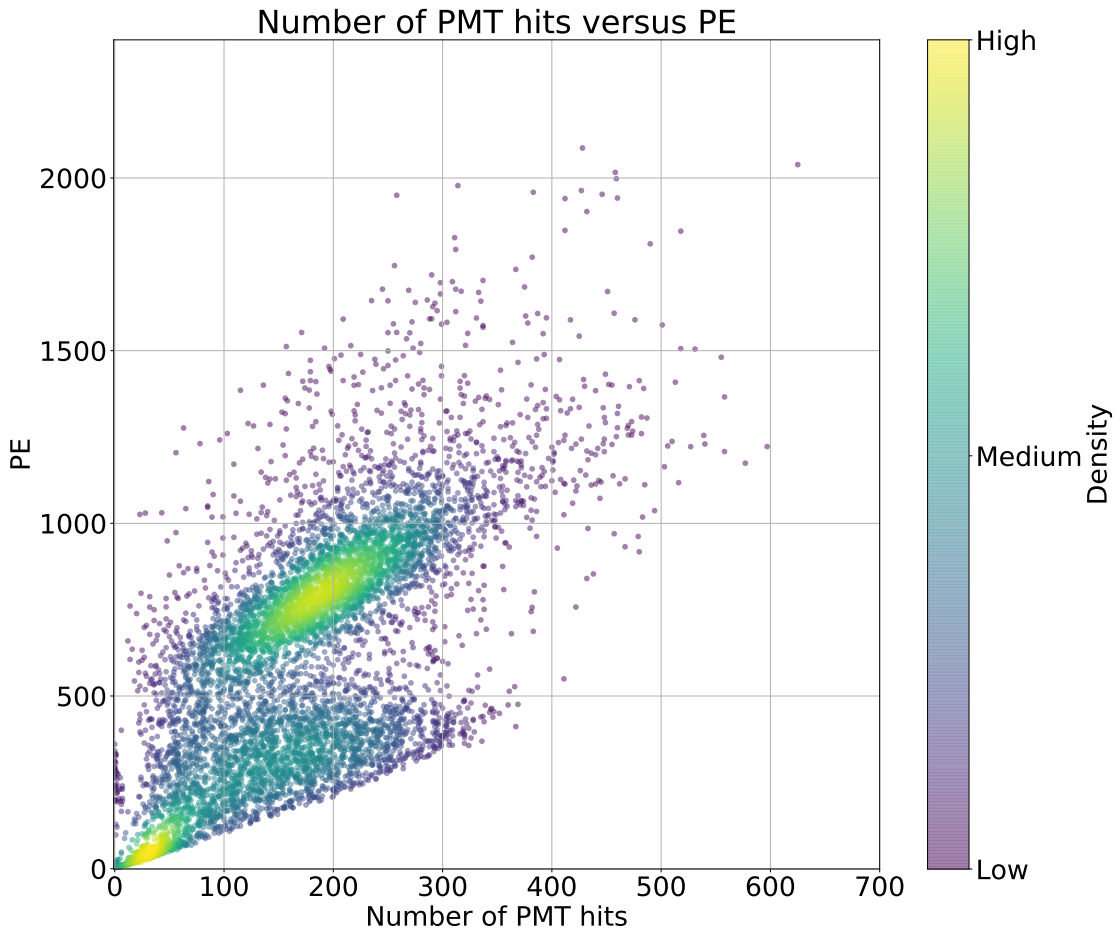

Figure 3.13: Number PMT hits per event versus number of p.e. per event.

The total number of PMT hits per muon including dark noise is shown in Figure 3.14.

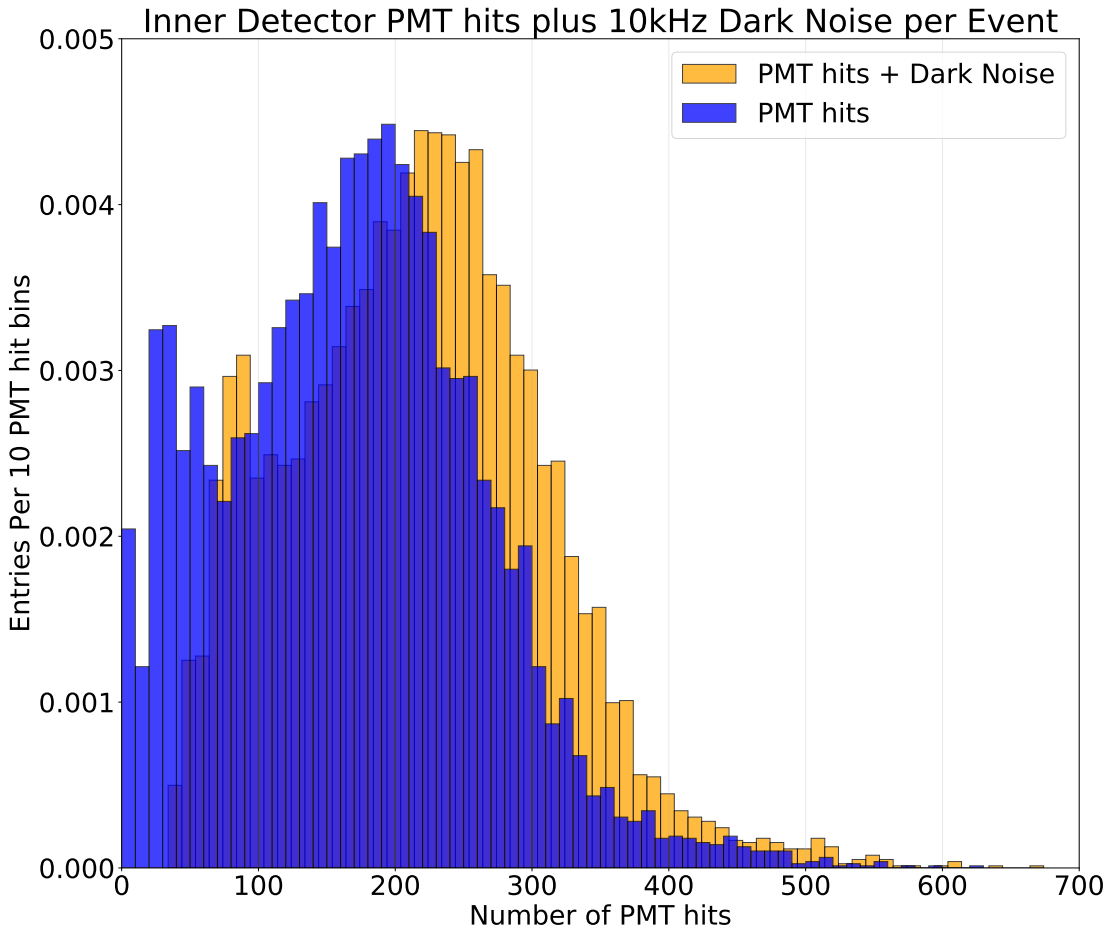

Figure 3.14: Number of PMT Hits per muon event plus 10 kHz Dark Noise rate.

CHAPTER 4
WATCHMAN DAQ REQUIREMENTS

There are two elements that dictate the WATCHMAN DAQ requirements. The first driver is the intrinsic dark noise rate of the PMTs. Based on measurements from a sample of 100 PMTs, the expected noise rate when submerged in water should be around 3 kHz [3]. The expected dark rate of 3 kHz due to the temperature of the water being colder than the ambient temperature. For a trigger system that requires four or more PMTs to register a hit within a 100 ns time window, with noise following a Poisson distribution, the trigger rate will be approximately 15 kHz. Based on simulations such as the ones shown in the previous chapter, WATCHMAN will detect about nine photoelectrons (p.e.) per MeV of deposited energy [3]. A summary of the DAQ requirements is shown in Table 4.1.

Table 4.1: Summary of important DAQ system requirements based on PMT gain of 10^7 [3]

Single Photoelectron Threshold	0.25 p.e.
Time Resolution	1.0 ns
Dynamic Range	12 bits
Trigger Threshold	4 hits in 100 ns
Maximum average PMT noise rate	10 kHz

The second important element is the rate of cosmic ray muons. Downward-pointing muons enter the detector with an estimated rate of .01 Hz. The main difficulty is the large amount on photoelectrons, around 20,000, that are generated in the PMTs [3]. These muons must be identified in order to remove them as a background. This forces the DAQ system to be sensitive to single photoelectron hits from IBD events to a large number of p.e. from a muon, requiring a large dynamic range.

CHAPTER 5
TARGET FMC PROTOTYPE DESIGN

5.1 DAQ System Overview

The WATCHMAN DAQ system requirements drive the overall system design. The main requirements revolve around the ability to resolve a single p.e. per signal. The system should be able to make a trigger decision and have no deadtime. Moreover the system should have the capability of extracting essential features of a signal for event building, such as the leading-edge time and amplitude, and transmit that information through Ethernet. The DAQ system has four main components: (I) the TARGETC ASIC as an analog to digital converter, (II) analog gain stages, (III) a trigger system, and (IV) a FPGA to serve as a controller. A readout system called the TARGETC FMC Prototype was designed to demonstrate a working solution for the WATCHMAN DAQ shown below in Figure 5.1.

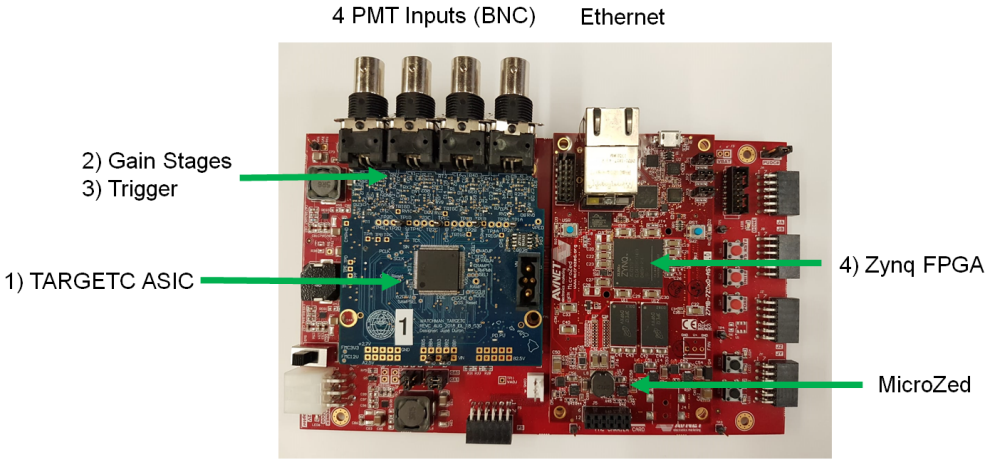

Figure 5.1: TARGETC FMC Prototype (blue) mounted along with MicroZed on a FMC Carrier Card (red)

The prototype readout card is designed to instrument 4 PMTs. Each PMT signal is sent through four analog gain stages in parallel. The four groups of x4 gain stage outputs are then connected to a TARGETC ASIC for analog-to-digital conversion. From the gain stages a copy is also sent to the trigger system, to determine if a hit occurred. The DAQ system utilizes a MicroZed [16], which has a combination of a processor and FPGA, to communicate with the TARGETC and process the outputs from the trigger system. Finally the system processes the waveform by time-stamping the hit and calculating the peak voltage before sending the it to an event builder through Ethernet. In Figure 5.2 the full signal path of the TARGETC FMC Readout System is shown.

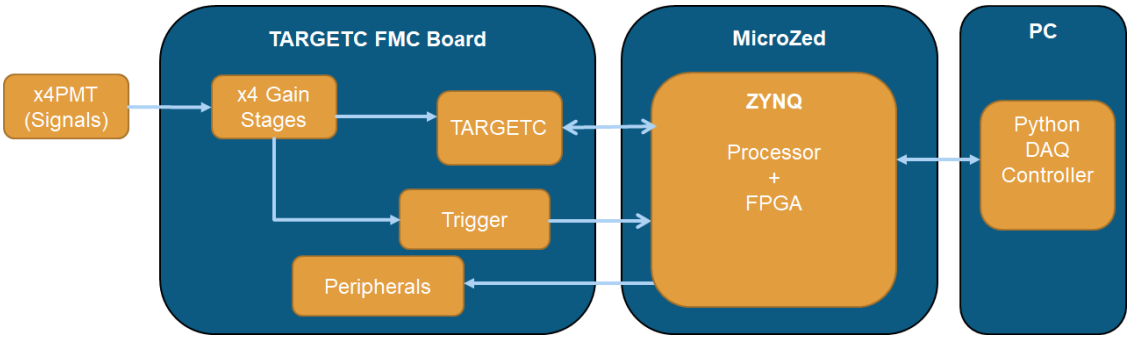

Figure 5.2: Signal flow overview for the TARGET FMC Prototype.

5.2 TARGETC as Analog to Digital Converter (ADC)

The analog to digital conversion is done by the TARGETC ASIC. TARGETC is a 16 channel, 1 Giga-sample per second waveform sampler, which includes a Wilkinson ADC. The usable input range of the TARGETC is from .5 V to 2 V is continuously sampling into an analog capacitor array but will only digitize groups of samples when triggered. The TARGETC has internal and random-access storage controlled by the FPGA, allowing the system operate deadtime-less. This internal storage is constructed by 512 addressable windows each holding 32 nanoseconds of analog waveform data. The whole buffer can therefore store up to 16 microseconds of waveform data per channel. Samples on all channels are digitized and read out simultaneously. Up to 4 PMTs can be connected to a single TARGETC. Monte Carlo simulations were carried out to demonstrate the capacity of the TARGETC to handle 4 PMTs at 10 kHz trigger rate.

5.2.1 Simulation for TARGETC memory buffer

In order to demonstrate the feasibility of the TARGETC as a solution that meets DAQ requirements, a comprehensive simulation was carried out. One of the main concerns of the readout system is the ability to handle a high trigger rate. A Monte Carlo simulation was developed to determine how the TARGETC would respond with four PMTs at its inputs. For this simulation the dominating trigger rate source comes from the dark noise of the PMTs. 10 kHz was the rate specified for the noise rate of each PMT. A virtual circular buffer was implemented based on how much space is available in the TARGETC internal memory buffer. The simulation takes into account how long it will take to digitize and transmit the data into the FPGA. The readout rate was specified at 24 microseconds. The percentage utilization of the memory buffer over time is shown in the upper plot of (Figure 5.3). The lower plot in this figure is a histogram of the frequency of the utilization of the memory buffer.

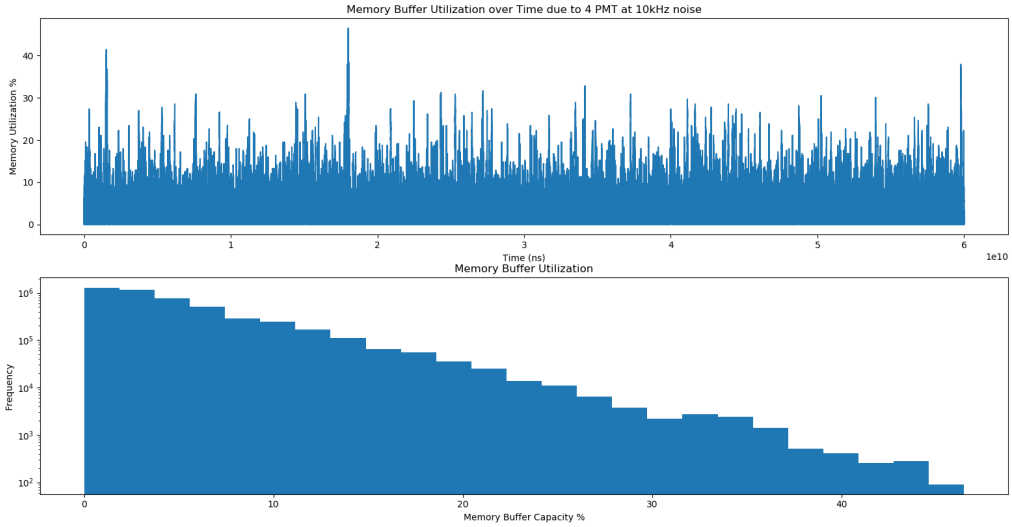

Figure 5.3: Occupancy simulation of the TARGETC internal memory buffer for the case of 4 PMT inputs each producing 10 kHz of dark noise rate.

This simulations demonstrate that the TARGETC buffer utilization is generally well-below 100% utilization. This means that the system is capable of digitizing every hit, without deadtime for the TARGETC with 4 PMTs at a rate of 10 kHz. This is important as the DAQ system needs to be able to digitize every hit from the PMT, to feed the reconstruction process of an IBD event.

5.3 Gain Stages

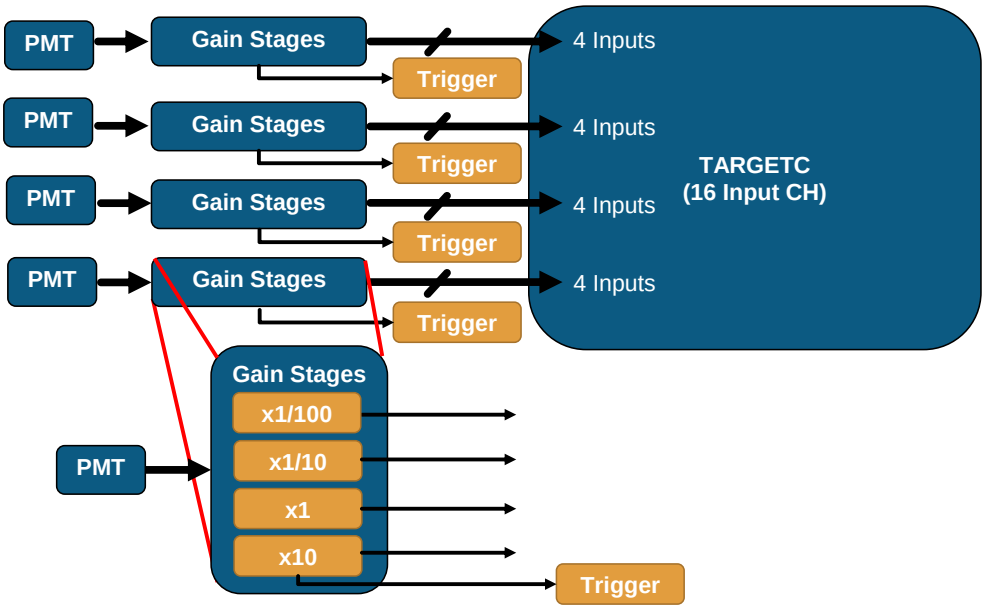

Figure 5.4: Each PMT output is connected to four amplification stages. The output for the x10 (V/V) stage is connected to the trigger system. A total of 16 channels, from 4 PMTs are connected to the TARGETC

Each PMT is an input to four separate gain stages, in order to increase the input dynamic range. Each input has a 50 Ohm impedance termination. The TARGET has a usable range of about 1.5 V. Pulses from the PMT can range from 10 mV for a single p.e. to 100 V for larger hits. The four stages have the gains (V/V): x10, x1, x1/10, x1/100 respectively as shown in Fig 5.4. A resistor divider circuit is used for all stages but the amplifier stage.

For the x10 gain stage a non inverting amplifier is used, AC coupled on the input and output. It is driven by a single supply of 4 volts. The amplifier used is the Texas Instruments LMH6629 selected for its high bandwidth, low noise and low power consumption. There is an isolation circuit before the amplifier to protect it from large voltage pulses that would damage the amplifier as shown in Figure 5.5.

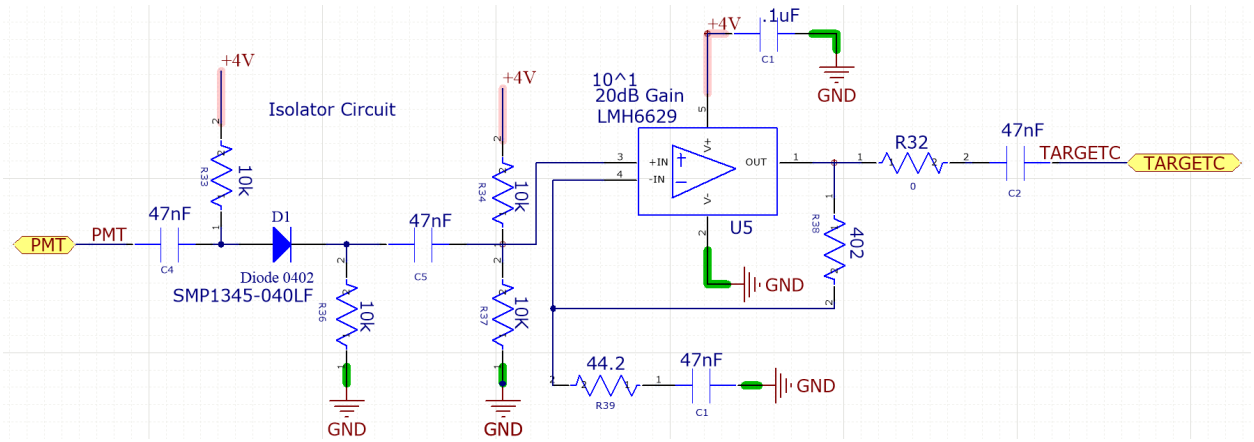

Figure 5.5: LMH6629 Amplifier Schematic Circuit for x10 gain stage.

5.4 Trigger System

The trigger mechanism consists of four Analog Devices ADCMP601 comparators, each connected to the output of an amplification stage, one per PMT input. When a pulse amplitude exceeds a set threshold, the comparator fires a trigger output signal. It was chosen for its fast rise time and small propagation delay. This comparator is CMOS compatible and it can be driven by single supply of 2.5 V. When any of the PMTs have a pulse, the FPGA will be able to receive the trigger signal, determine which PMT was triggered, and create a signal for the TARGETC to start digitizing. The threshold for the trigger is controlled by a digital-to-analog converter (DAC).

5.5 MicroZed - Zynq-based System-on-Module

The TARGETC FMC readout module employs a MicroZed Board as a controller. The MicroZed is a commercially available System-On-Module (SoM) with a Xilinx Zynq-based FPGA. It has several useful built-in features, like 1 gigabyte of RAM, an SD card reader, an Ethernet port, a UART interface and easy access to 100 I/O pins. The MicroZed is powered by a 5 volt single supply. An FMC Carrier Card was used to connect the TARGETC FMC board and the MicroZed.

The main feature of the MicroZed board is the Zynq FPGA. The Zynq architecture combines a FPGA with an ARM processor. The Zynq receives trigger inputs, generates clocks, controls and collects data from the TARGETC. The Zynq subtracts pedestals and compresses the waveform data by extracting the charge and timing information of a pulse. Data are then streamed through an Ethernet link into an event builder.

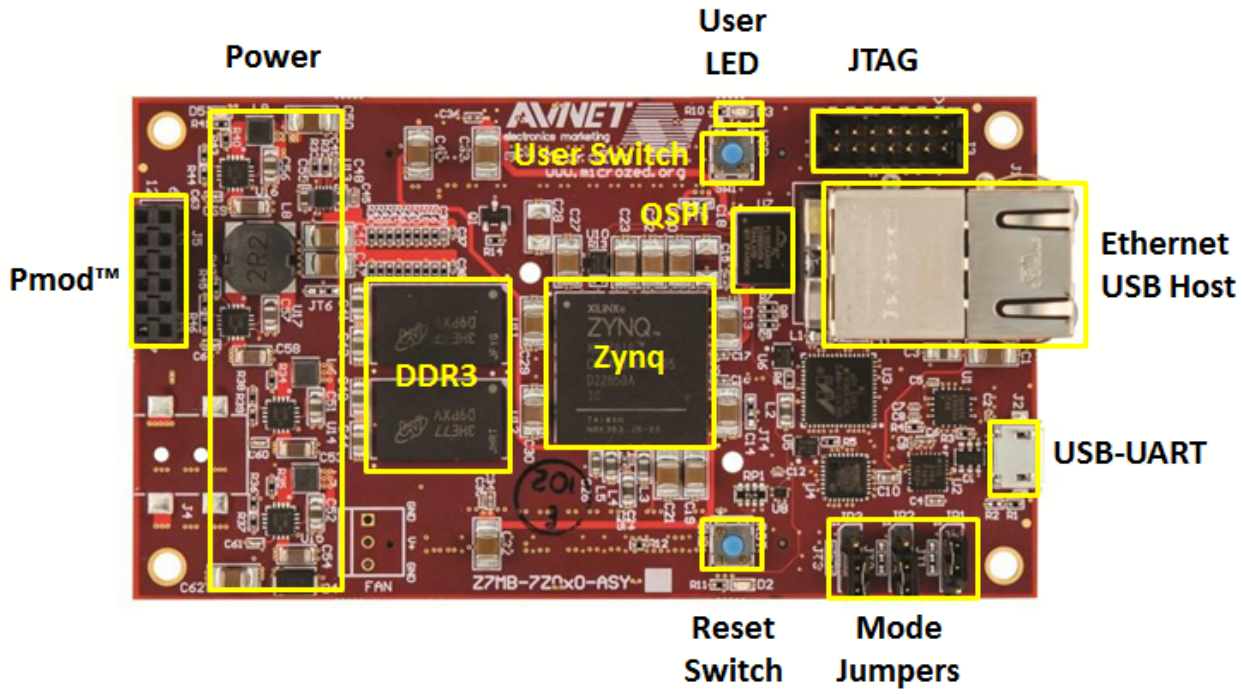

Figure 5.6: A photograph of the MicroZed Board's essential hardware components [16].

5.6 Software Overview

Software and firmware had to be developed in order to test and operate the WATCHMAN DAQ system. There are three components that were developed for the readout system. A python-based application was developed to handle all communication to and from the TARGETC FMC Prototype through Ethernet using the User Datagram Protocol (UDP). Embedded software was developed for the ARM Processor that initializes the prototype system on power-up, opens an Ethernet channel which it uses to send waveform data, as well as receive and processes commands. The firmware developed for the FPGA is responsible for the handling of the TARGETC interfaces, as well as the peripherals and trigger signals. Together the three components are able to process a trigger from a PMT signal, sample and digitize the waveform, send the data to the processor and sent through Ethernet (see Figure 5.7).

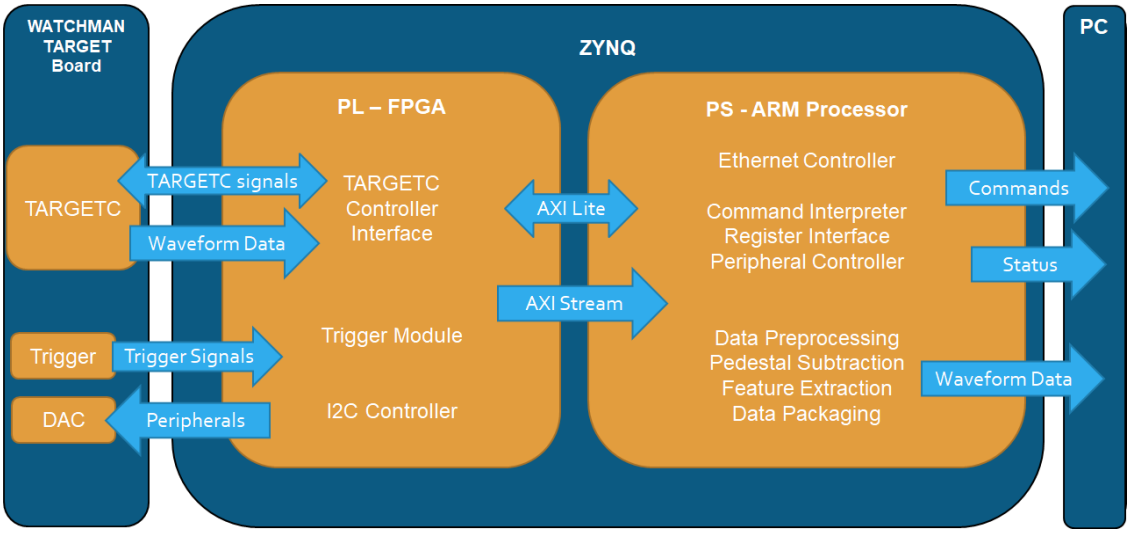

Figure 5.7: Signal Flow for TARGET FMC Prototype

5.6.1 Python DAQ Controller

The Python DAQ Controller (PyDAQ) is an application that handles all the communication to and from the TARGET FMC Prototype. All communication is carried out through Ethernet using User Datagram Protocol (UDP). The main task for PyDAQ is to create and maintain a (UDP) socket. This includes setting up an IP address and port number for sending and receiving UDP packets. An IP address is defined and two ports are set up. There are two types of communication: slow control and waveform data. Slow control commands are sent to the TARGET FMC Prototype or status messages received from the system. Data flows only in one direction, from the readout system.It can be either full waveform data or feature-extracted waveform data. Two communication protocols were developed for sending and receiving packets between PyDAQ and TARGET FMC.

The slow control protocol is used to send commands to from the PyDAQ to the TARGET FMC Prototype and it can be used to to receive messages as a way of monitoring the readout system. Several commands were designed, the most important ones pertain to reading and writing registers as well as selecting an operation mode for the system. There are many registers that need to be configured, both for the TARGET ASIC as well as for the readout system. One of the limitations of UDP is the inability to know if a package was received. When the readout system receives a command it echos the package back to the PyDAQ as an acknowledge that the command was indeed received.

The waveform data protocol only works in one direction, from the TARGET FMC Prototype to the PyDAQ. One significant drawback of UDP is that if the data is sent out and was not received it is lost and the PyDAQ has no way of knowing that a packet was lost. PyDAQ converts the data received into a a text file.

5.6.2 PS - ARM Processor

The ARM processor handles all Ethernet communication to and from the PyDAQ and has to interface with the FPGA part of the Zynq. A custom embedded software was developed to run on the processor. The main functions of this software are creating maintaining a UDP connection for sending and receiving commands as well as packaging and sending out waveform data. The processor must be able to interpret and process the commands accordingly.

Two interfaces are used to communicate between the FPGA and the processor. The AXI Lite interface for slow communication and AXI Stream for fast data transfers. The slow communication channels are used for sending register settings and commands to the FPGA. This AXI Lite interface is bi-directional and can be used to receive status information. The AXI Stream interface only sends data from the FPGA to the RAM, which the processor has direct access to.

Lastly the waveforms are processed and package before they are sent out. The processor has the ability to calculate pedestals and perform pedestal subtraction on the data. Pedestals refer to a constant offset that each sample has due to the variation from the storage cells in the TARGETC ASIC. The processor can also generate a transfer function and correct for non-linear behavior of the TARGETC. Additionally the processor can, for simple waveforms, extract the charge and the timestamp. The processor will package this data into a predefined structure inside a UDP package and send it through the Ethernet interface.

5.6.3 PL - FPGA

The FPGA's primary function in the TARGET FMC Prototype is to interface with all the front-end electronics, namely the TARGETC, the comparators, and the DAC. Additionally, the FPGA must be able to communicate with the processor, to be able to receive and interpret commands, as well as be able to send out the data received from the TARGETC. The FPGA also manages the DAC on the TARGET FMC board through an I2C controller.

The most complex system the FPGA has to interface to is the TARGETC. The TARGETC has three separate interfaces each with a custom protocol: a serial register interface, a sampling and writing interface, and a digitizing and readout interface. Additionally the FPGA has to provide three clocks for the TARGETC. A TARGETC controller firmware block was developed that manages all the functionality for the TARGETC input and output signals.

The TARGETC is constantly sampling, with the FPGA providing a clock and a address to store the analog voltage to an internal storage. The TARGETC's internal memory storage is random access and full control is given to the FPGA on how to manage it. Managing the memory storage efficiently is a crucial task at high trigger rates to avoid dead time or overwriting useful data. The FPGA is also responsible for receiving the raw waveform data from the TARGETC. The FPGA must be ready to receive and deserialize the data, package it and send it to the external RAM through an AXI Stream interface.

CHAPTER 6
RESULTS

6.1 TARGETC FMC 4 Channel Prototype

A test-bench was built for the TARGETC FMC Prototype. The software and firmware for the prototype board has been developed to run various tests. Several tests were carried out to calibrate, characterize and demonstrate the viability of the proposed design.

6.1.1 Linearity

The input range of the TARGETC was tested by scanning the DC level slowly and determining the region that behaves linearly, around 1 V to 2 V (see Figure 6.1). Data was taken by sweeping the DC baseline from 0V to 2.5 V in .01 V increments. 128 samples were taken for each voltage value. The mean of these samples and one standard deviation is shown. The data was fitted with a line from 1 V to 2 V. The linear fit falls within 1 standard deviation of the data.

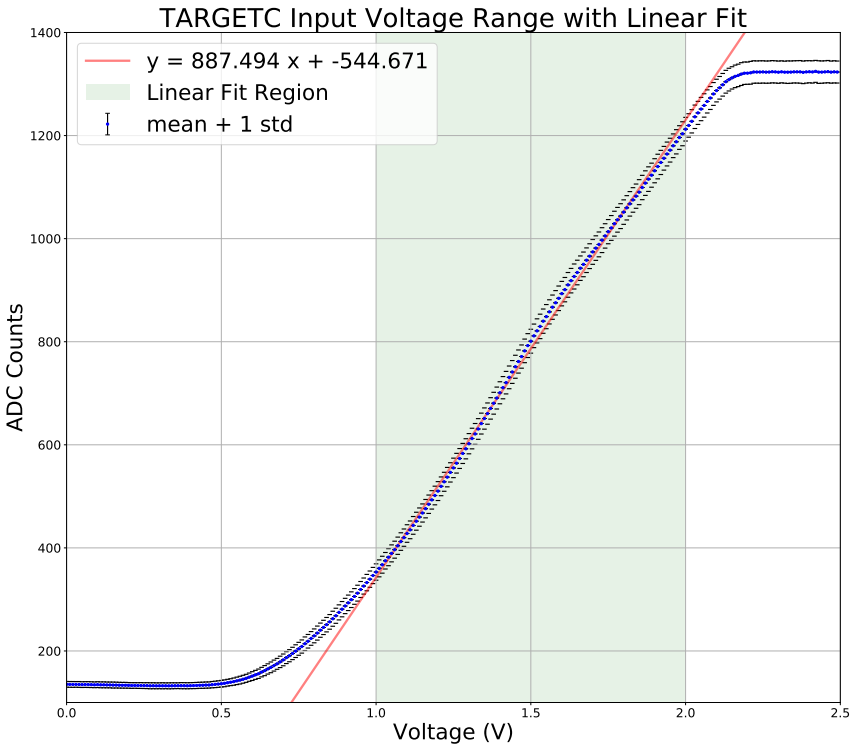

Figure 6.1: TARGETC measured ADC counts versus input DC voltage with linear fit superimposed.

The difference between the data and the fit was calculated, as well as the relative error. With the residuals and the linear fit, it is possible to account for the non-linearity of the TARGETC within the bounds of 1 V and 2V.

6.1.2 Noise Measurements - Pedestals

The TARGETCs waveform data has an intrinsic offset due to the slight variations in the storage cells from one capacitor to the next. In order to account for this offset, several samples of data are taken and then averaged and subtracted from the waveform data. The pedestal subtracted data should now be centered around zero with small variations (see plot 6.2). A Gaussian fit of the histogram of the pedestal values for all the buffer is shown in Figure 6.5. The mean offset for all samples was .255 mV with a standard deviation of 1.351 mV. The non-uniformity is due to a known quantization error in the Wilkinson ADC.

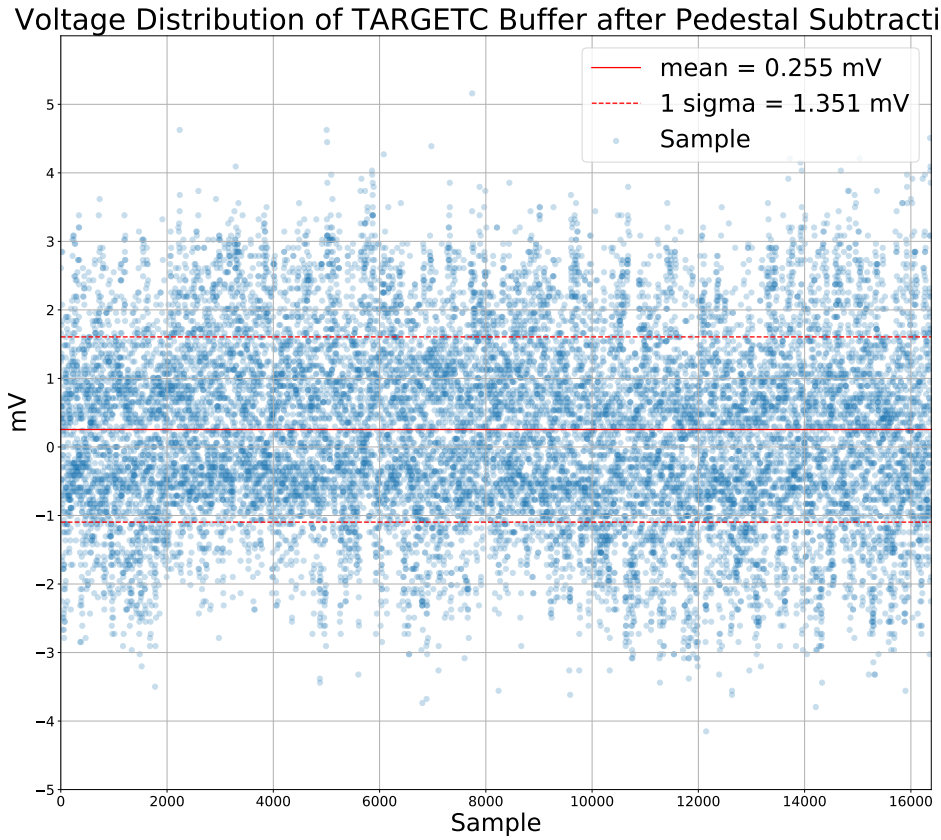

Figure 6.2: Pedestal Subtracted residuals for all samples (512 windows x 32 samples/window.

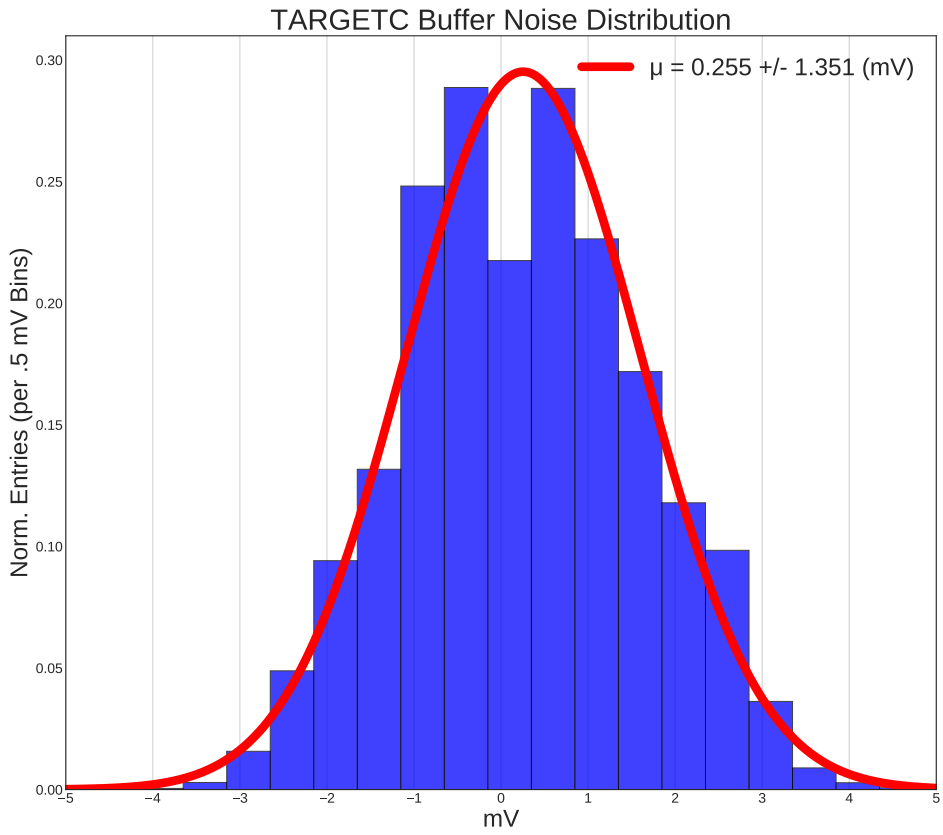

Figure 6.3: Gaussian fit of histogram of pedestal subtracted data for all windows.

6.1.3 Timing Resolution

To test the timing resolution, a function generator was used to output a 29 MHz sine wave. The sample waveform data was then fitted to find the period (Figure 6.4). To obtain statistics, 100 sine wave samples were taken. The residuals from the period extracted from the fit were calculated. These residuals are plotted in a histogram in Figure 6.5. The difference from the source on the period over 100 samples was 54 picoseconds, with a standard deviation of 96 ps.

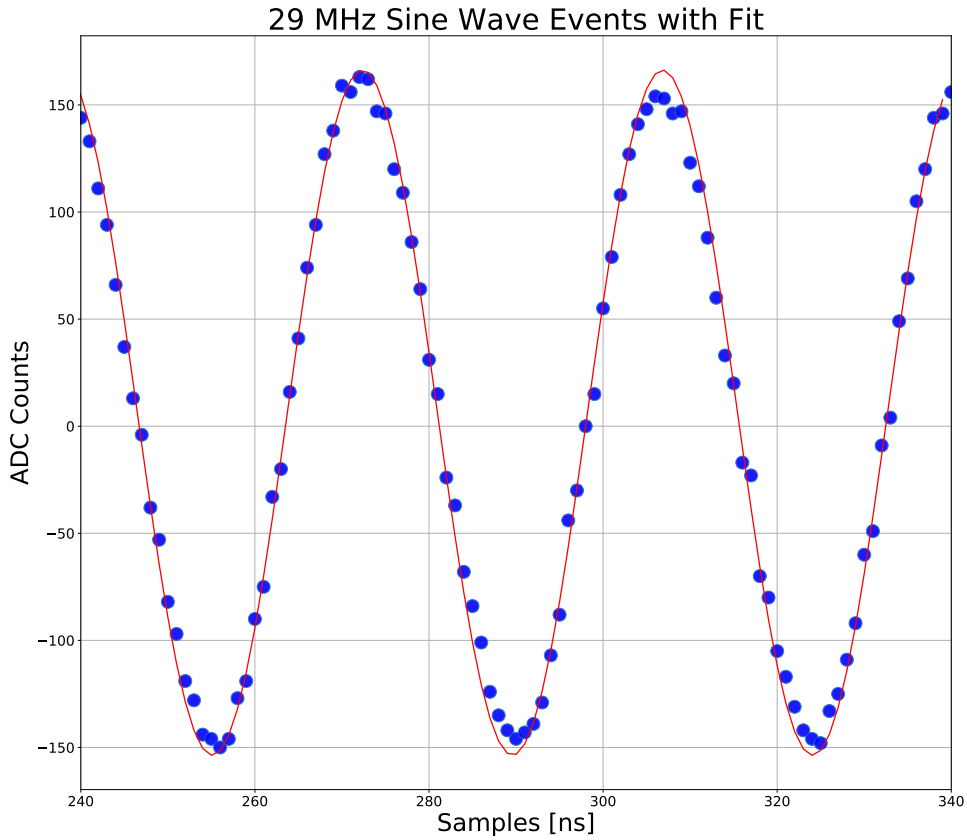

Figure 6.4: A 29 MHz sine wave sample waveform with fit superimposed.

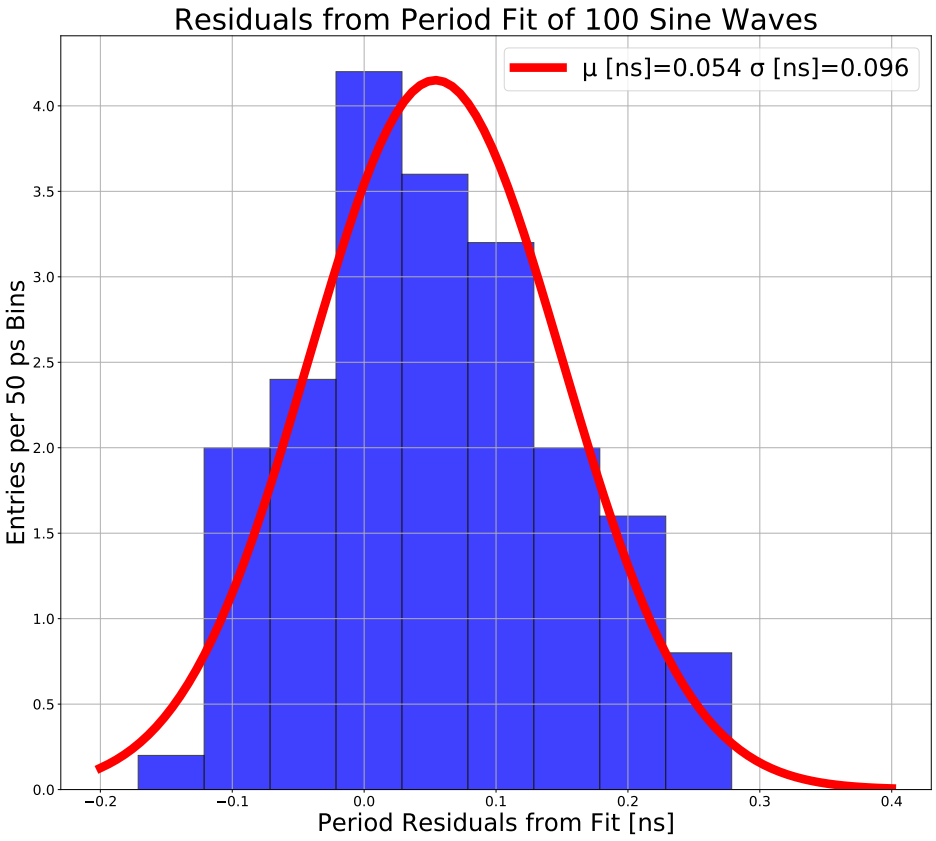

Figure 6.5: Histogram of Residuals from fitting to a period of 29 MHz sine wave.

6.1.4 PMT-Like Pulse

A PMT output signal has a rise time of around 3 ns. For testing purposes a function generator was used as a pulse source to simulate a PMT pulse. A 3 ns rise time pulse was digitized at at 1 giga sample per second sampling (see figure 6.6).

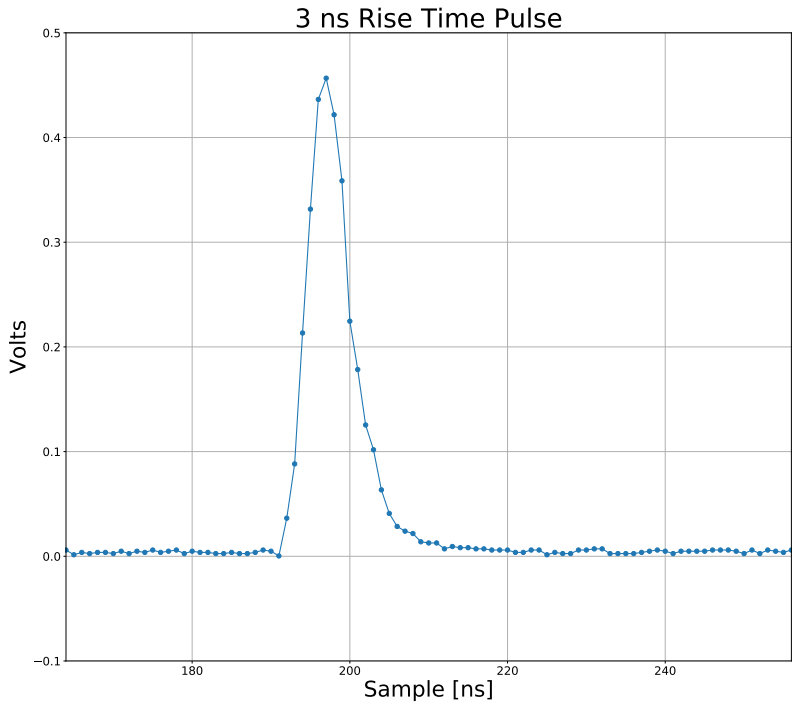

Figure 6.6: 3 ns risetime pulse recorded with the TARGET FMC Prototype.

6.1.5 Linearity of Pulse Height versus Area

Due to the high single p.e. rates per readout board, it is necessary to compress the waveform data to reduce the data volume. The readout system must be able to compress a pulse by extracting and transmitting the pulse height and time instead of the full waveform data. A sweep of 99 pulses, each of 3 ns risetime, with increasing amplitudes were generated by a function generator. The sweep started at 6 mV amplitude with 6 mV increments, until the maximum amplitude of 600 mV. The relationship between the sampled pulse's height and its area is shown in Figure 6.7.

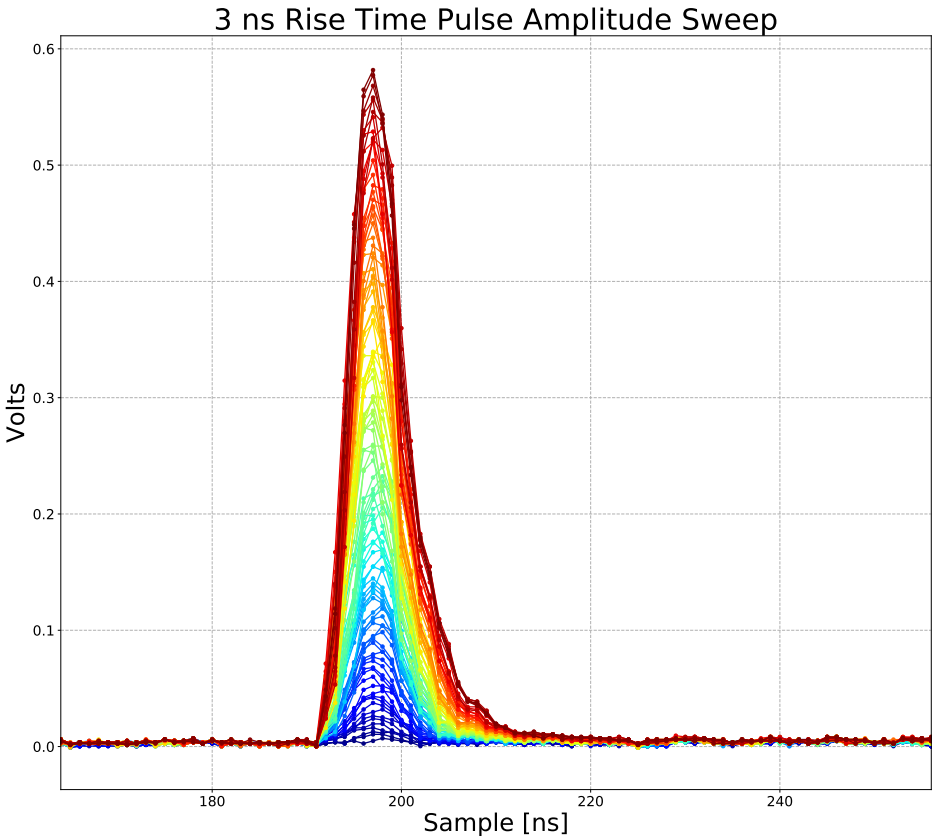

Figure 6.7: 3 ns risetime pulse sweep with increasing amplitude.

The maximum of every pulse was extracted and the area of the pulse was calculated. To find the area the integral was approximated using trapezoidal approximation. The pulse height is plotted against the area with a line is fitted against the data. The residuals are also calculated and plotted versus the pulse height (see Fig. 6.8).

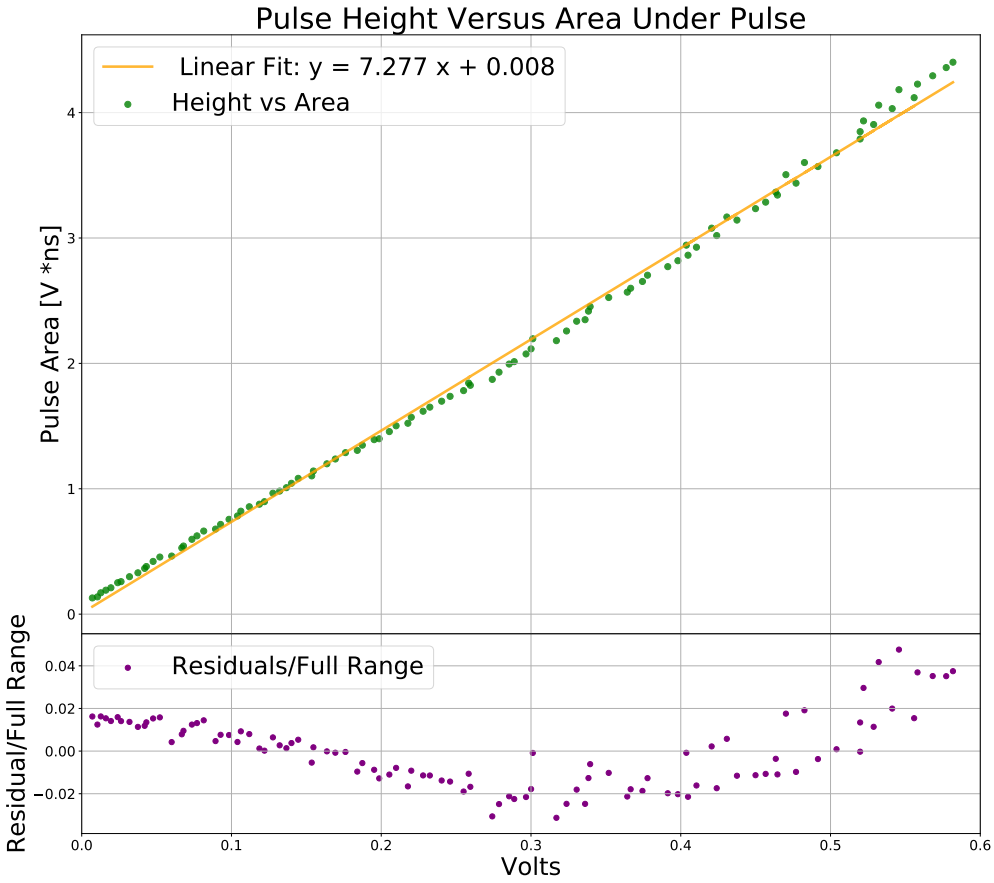

Figure 6.8: Pulse height versus area with linear fit.

CHAPTER 7
FUTURE WORK

7.1 TARGET VME DAQ

For economic reasons, the WATCHMAN detector requires a high channel density DAQ. The FMC prototype with only 4 PMT inputs is not ideal when there are around 3600 PMTs in the WATCHMAN detector. For this reason, the channel number must be increased to sixteen PMT inputs per DAQ board. For convenience, the board should use VME standards to draw power from standard VME crates. The PMT inputs will be fed through a Rear Transition Module (RTM) through the VME backplane. The main design components for the TARGET VME board will be the same, or very similar to the prototype board. There will be two MicroZed boards, each connected to two TARGETCs with 4 PMTs each (see Figure 7.1 below). The design of this readout system is heavily based on the TARGET FMC Prototype board.

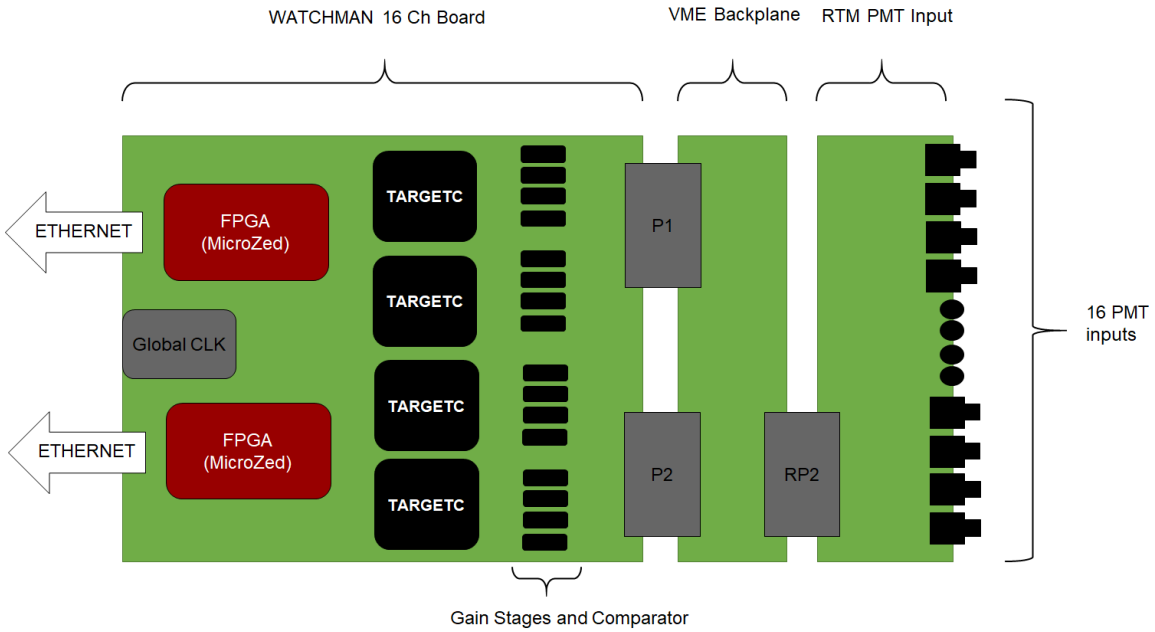

Figure 7.1: Diagram of one set of boards of the TARGET VME DAQ system with VME Backplane and RTM.

7.2 Secondary Trigger System

The trigger system will use the same comparators as the TARGET FMC Board, and will also have an additional trigger mechanism. Four outputs of the amplifier stage from each PMT will be added using a summing amplifier. The summing amplifier will be a unity gain inverting amplifier that employs Analog Devices' LTC6252 as the operational amplifier. The output of the summing amplifier is connected to a balun transformer that serves as a single to differential pair converter.

This differential pair analog signal will be sent to a 250 mega samples per second analog-to-digital converter. The HMDCAD511 from Analog Devices will be used as the ADC. By sending the digitized waveform of the sum of the PMT channels, the FPGA can determine if there is a pulse or not. This creates a secondary trigger signal. This signal is useful in cases where the comparators are constantly firing due to baseline fluctuations. In order to be as sensitive as possible to single p.e. hits, the comparator threshold will be set as low as possible. Setting the threshold close to the baseline may cause a false trigger when there is no pulse. Having a secondary triggering mechanism overcomes this issue. A diagram of the secondary trigger mechanism is shown below (Figure 7.2).

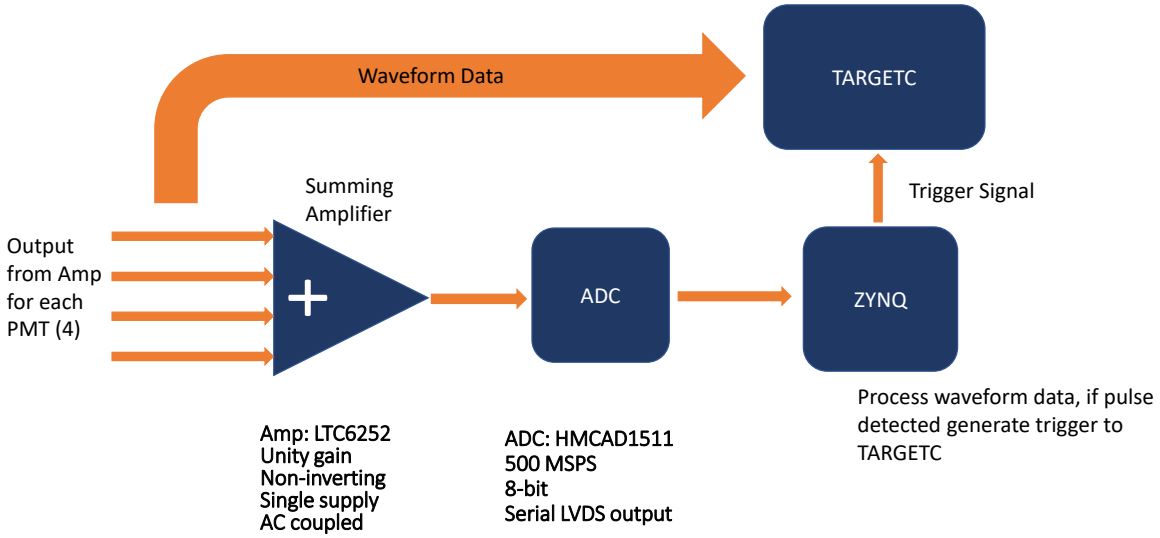

Figure 7.2: Trigger System using Analog Devices' HMDCAD511 as an ADC to provide a secondary triggering mechanism

7.3 Global Sync Clock

Precise timing is very important for reconstruction of physics events. For the WATCHMAN DAQ system, it is required that the readout system can be synchronized to an external clock. The TARGET VME DAQ will have access to an external clock signals that can be used to synchronize all of the DAQ systems with a global clock.

7.4 MicroZed as a controller for 2 TARGETCs

The idea for reusing the MicroZed is to speed up the development time for the firmware and software. By using the same system-on-module, most of the firmware and software can be reused in this system. The main difference is that one MicroZed must control two TARGETCs independently, but the assumption is that the firmware development should be straightforward as the next step from the prototype version. In a similar sense all the I2C peripherals that were controlled by the FPGA on the TARGET FMC Prototype will be controlled directly by the processor. The TARGET VME DAQ will use a switch to hardware encode a unique IP address that will be used by each MicroZed in order to have unique static IP addresses.

7.5 TARGET VME DAQ 3D Rendering

The TARGET VME board was fabricated and assembled. Below is a 3D rendered view with the MicroZeds and the TARGETs labeled in Figure 7.3. As soon as the software and firmware is sufficiently developed, this will be the board that should be considered as a readout system that can to meet WATCHMAN DAQ requirements.

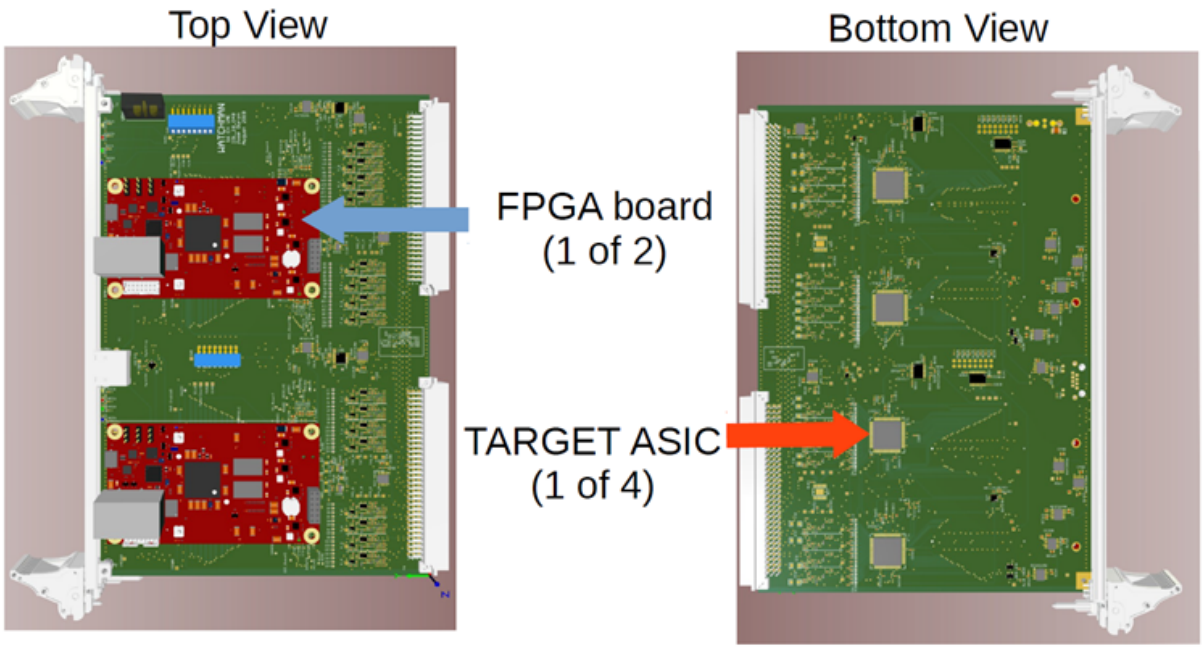

Figure 7.3: 3D rendering of the TARGET WATCHMAN DAQ board

CHAPTER 8
DISCUSSION

TARGET VME DAQ fulfills all the WATCHMAN requirements and is an adequate readout system solution. Simulations of IBD and muon events were carried out using RAT-PAC. DAQ system requirements were derived from the results from these simulations. A design of a readout system that would meet these characteristics resulted in the TARGETC FMC Prototype. Testing of the TARGETC FMC Prototype was carried out and discussed. Development of the next stage in the readout system resulted in the TARGET VME DAQ. The TARGET VME DAQ should be sufficiently equipped to handle the design specifications required for the WATCHMAN readout electronics.

Table 8.1: Summary of TARGET FMC Prototype Characteristics

Sampling Rate	1 giga sample per second
Time Resolution	100 ps
Input Voltage Range (DC)	1 V to 2 V
Noise Level	$\pm$1.35 mV

Simulations of the TARGETC ASIC internal memory storage demonstrate the ability to sustain trigger rates up to 40 kHz without deadtime. The TARGETC FMC Prototype has a wide dynamic input range due to its four gain stages, allowing signals from 100 V to 10 mV to be sampled within the usable input range of the TARGETC. The 16 channel TARGET VME DAQ system has all these characteristics and with an improved trigger mechanism which allows reliable triggering on single p.e. hits. TARGET VME DAQ meets or exceeds all the requirements that would make an ideal readout electronics system for the WATCHMAN detector.

APPENDIX A
HAWAII WATCHMAN TEAM MEMBERS

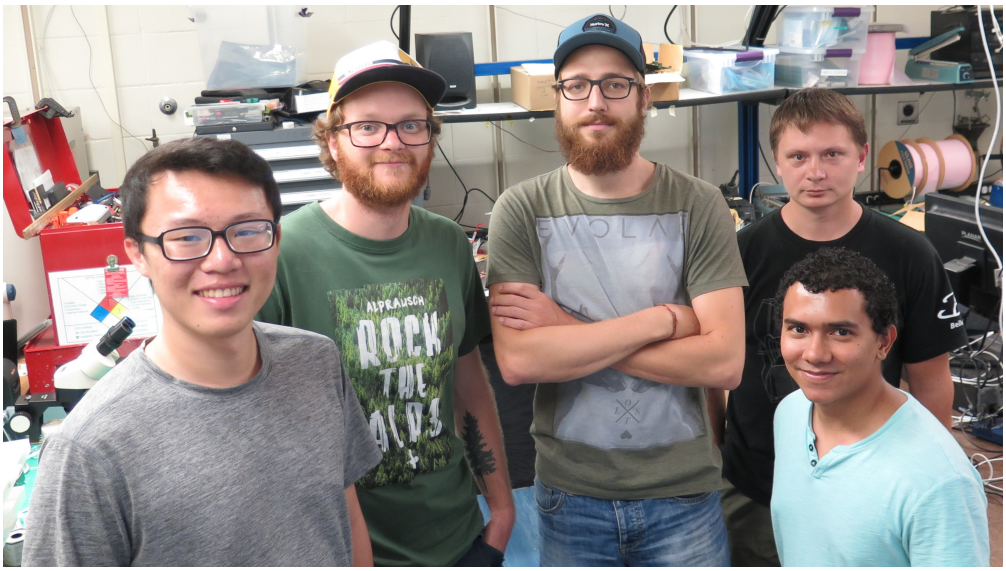

Figure A.1: The WATCHMAN IDLAB team members from left to right: Ky Ho, Jonathan Hendriks, Anthony Schluchin, Vasili Shebalin, Jose Duron

Figure A.2: The newest WATCHMAN IDLAB member: Salvador Ventura

BIBLIOGRAPHY

[1] M Askins, M Bergevin, A Bernstein, S Dazeley, ST Dye, T Handler, A Hatzikoutelis, D Hellfeld, P Jaffke, Y Kamyshkov, et al. The Physics and Nuclear Nonproliferation Goals of WATCHMAN: A WAter CHerenkov Monitor for ANtineutrinos. *arXiv preprint arXiv:1502.01132*, 2015.

[2] Thierry Lasserre and Henry W Sobel. Reactor Neutrinos. *Comptes Rendus Physique*, 6(7):749–757, 2005.

[3] A Bernstein. AIT-WATCHMAN Conceptual Design Review Report. Technical report, Lawrence Livermore National Lab.(LLNL), Livermore, CA (United States), 2019.

[4] KamLAND& Eguchi, S Enomoto, K Furuno, J Goldman, H Hanada, H Ikeda, K Ikeda, K Inoue, K Ishihara, W Itoh, et al. First Results from KamLAND: Evidence for Reactor Antineutrino Disappearance. *Physical Review Letters*, 90(2):021802, 2003.

[5] Yu-Feng Li. Overview of the Jiangmen Underground Neutrino Observatory (JUNO). In *International Journal of Modern Physics: Conference Series*, volume 31, page 1460300. World Scientific, 2014.

[6] FP An, JZ Bai, AB Balantekin, HR Band, D Beavis, W Beriguete, M Bishai, S Blyth, K Boddy, RL Brown, et al. Observation of Electron-Antineutrino Disappearance at Daya Bay. *Physical Review Letters*, 108(17):171803, 2012.

[7] Sea Agostinelli, John Allison, K al Amako, John Apostolakis, H Araujo, P Arce, M Asai, D Axen, S Banerjee, G 2 Barrand, et al. GEANT4 - a Simulation Toolkit. *Nuclear instruments and methods in physics research section A: Accelerators, Spectrometers, Detectors and Associated Equipment*, 506(3):250–303, 2003.

[8] S Siebert. RAT-PAC. https://rat.readthedocs.io/en/latest/overview.html.

[9] Xin Qian and Jen-Chieh Peng. Physics with Reactor Neutrinos. *Reports on Progress in Physics*, 2018.

[10] Masaharu Tanabashi, K Hagiwara, K Hikasa, K Nakamura, Y Sumino, F Takahashi, J Tanaka, K Agashe, G Aielli, C Amsler, et al. Review of Particle Physics. *Physical Review D*, 98(3):030001, 2018.

[11] Rachel Erin Carr. *Measurements of Electron Antineutrino Disappearance in the Double Chooz Experiment*. PhD thesis, Columbia University, 2015.

[12] Hamamatsu. *"Large Photocathode Area Photomultiplier Tubes"*, 3 2019.

[13] Pablo Fernández Menéndez. *Neutrino Physics in Present and Future Kamioka Water-Čerenkov Detectors with Neutron Tagging*. Springer, 2018.

[14] Glenn Horton-Smith. GLG4sim. http://neutrino.phys.ksu.edu/∼GLG4sim/.

[15] Michael Smy. Low Energy Event Reconstruction and Selection in Super-Kamiokande-III. In *Proceedings, 30th International Cosmic Ray Conference (ICRC 2007): Merida, Yucatan, Mexico, July 3-11, 2007*, volume 5, pages 1279–1282, 2007.

[16] MicroZed. http://www.zedboard.org/product/microzed.